Optimization of Process Parameters During Multipass Metal Inert Gas Welding of SS 304 Stainless Steel

A Dissertation Submitted

in partial fulfillment of the requirements for
the degree of

Master of Engineering
in
Production Engineering

by

Rohit Chopra
(801382021)

Under the Supervision of
Dr. Ajay Batish
Professor

MECHANICAL ENGINEERING DEPARTMENT

THAPAR UNIVERSITY, PATIALA

July, 2015

CERTIFICATE

I hereby declare that the thesis entitled **"Optimization of Process Parameters During Multipass Metal Inert Gas Welding of SS 304 Stainless Steel"** is an authentic record of my work carried out as requirements for the award of the degree of **Master of Engineering** in **Production Engineering** at **Thapar University, Patiala** under the supervision of Dr. Ajay Batish, Professor, Mechanical Engineering Department, Thapar University, Patiala during July, 2013 to 15 July, 2015. No part of the matter embodied in this report has not been submitted to any other university or institute for the award of any degree.

Date: 25-7-2015

Rohit Chopra

Rohit Chopra

It is certified that the above statement made by the student is correct to the best of my knowledge and belief.

Dr. Ajay Batish
Mechanical Engineering Department
Thapar University, Patiala – 147004

Countersigned by

Dr. S.K. Mohopatra
Head, Mechanical Engineering Department
Thapar University, Patiala – 147004

Dr. S.S Bhatia
Dean of Academic Affairs
Thapar University,Patiala - 147004

Acknowledgement

I would like to thank all the people who contributed in some way to the work described in this thesis. First and foremost, I thank my thesis supervisor **Dr. Ajay Batish** for his guidance, support and inspiring suggestion, for the development of thesis at every step. He took keen interest in my report and allowed me to access facilities of Mechanical Engineering Department laboratories.

I would like to express my gratitude towards **Dr. Anirban Bhattacharya** for his essential valuable advice, positive, criticism, thoughts and constant encouragement through discussions. I am thankful to Mr. Narinder Singh for assisting and guiding me in laboratory work. I am thankful to MED faculty for support and guidance. Who took keen interest in my report and allowed me to access facilities of Mechanical Engineering Department laboratories.

I would also like to thank **Dr. S.K. Mohapatra, HOD, MECHANICAL DEPARTMENT** who motivated me to complete research work report with enthusiasm and hard work.

A special thanks to my friends Azad Kumar and Gaurav Talwar for their help and support during thesis work.

Rohit Chopra

Rohit Chopra
(801382021)

Abstract

Stainless steel is very popular in fabrication industry because of its excellent properties like high strength at low temperatures and corrosion resistance. It is used as structural material in nuclear reactors, valve bodies, chemical vessels, dairy industry and for carrying and storage of liquid nitrogen. Welding is important fabrication process used for processing of stainless steel. Quality of a joint is affected by the welding input parameters. In present study the effect of various MIG welding input parameters like voltage, current, gas flow rate, interpass temperature and groove angle were investigated. Effect of input parameters on distortion, impact toughness and microhardness of weld joint is studied. Mode of failure in fractured toughness samples is also investigated. Taguchi L18 orthogonal array was used for designing of experiment and results were analyzed by ANOVA. The responses measured in this study were charpy impact toughness test at room temperature and at -20˚C, Distortion in welds, microhardness at fusion zone and heat affected zone, microstructural study and SEM of fractured samples of impact testing. Microstructural study was done by optical micrographs. SEM images of fractured samples were used to find the mode of fracture.

Table of contents

List of Figures

List of Tables

Greek Symbols

η_{opt} ≡ Optimized value

Acronyms and Abbreviations

MIG	≡	Metal Inert Gas
TIG	≡	Tungsten Inert Gas
ANOVA	≡	Analysis of Variance
DOE	≡	Design of Experiment
DOF	≡	Degree of Freedom
HAZ	≡	Heat Affected Zone
SEM	≡	Scanning Electron Microscope
SS	≡	Sum of Squares
XRD	≡	X-Ray Differaction
NS	≡	Not Significant
S	≡	Significant
FEM	≡	Finite Element Modelling
FZ	≡	Fusion Zone
BM	≡	Base Metal
$\bar{m}$	≡	Mean of observations

Chapter 1

Introduction

1.1 Introduction

This chapter deals with introduction to welding, particularly metal inert gas welding (MIG) its principle, equipment, advantages and disadvantages. This chapter also discuss stainless steels, its types, properties and uses.

1.2 Welding

Welding is a fabrication process for permanent joining of two materials. Permanent joining of two or more materials with or without application of pressure, heat and filler material is called welding. In manufacturing industry welding is commonly used fabrication process. Arc welding was come into existence in the end of 18^{th} century. In arc welding processes electric arc is used as a heat source.

1.3 Metal Inert Gas Welding (MIG) or Gas Metal Arc Welding (GMAW)

In early 19^{th} century, MIG welding was developed as a solution to time consuming process of changing electrode pieces. In MIG welding continuous filler wire is used as electrode. MIG welding is a process where coalescence is produced by heating the workpiece with an arc struck between consumable bare wire electrode and workpiece. Arc is shielded by inert gases (He, Ar), active gases (CO_2) or mixture of gases. Feed of consumable electrode in this process is continuous so process can be semi-automatic or automatic, which is capable of providing high welding speed to meet demands of industries. [Weman and Lindean, 2006]

1.3.1 Principle of MIG Welding

MIG welding is an arc welding process which is consists of continuous feeding of consumable electrode, which is shielded by an inert, active gas or mixture of gases. This consumable electrode wire is fed through a nozzle. When electrode came in contact of workpiece short circuiting occurs, because of opposite polarity of electrode and work piece. Short circuiting results in heavy flow of current, which leads to high amount of heat

generation as shown in Fig. 1.1. This generated heat is capable of melting of electrode tip. Due to heating of electrode, it emits some free electrons. Vapour of metal also disassociate into ions due to their lower ionisation potential. On pulling the electrode away from workpiece the current starts flowing through charged particle and arc is developed. In gas metal arc welding the electrode also serve the purpose of filler metal too. Gas metal arc welding can be done with both direct current and alternating current. Commonly direct current electrode positive polarity (DCEP) is used in gas metal arc welding. In DCEP maximum heat is produced at electrode, which causes melting of electrode and arc cleaning action.

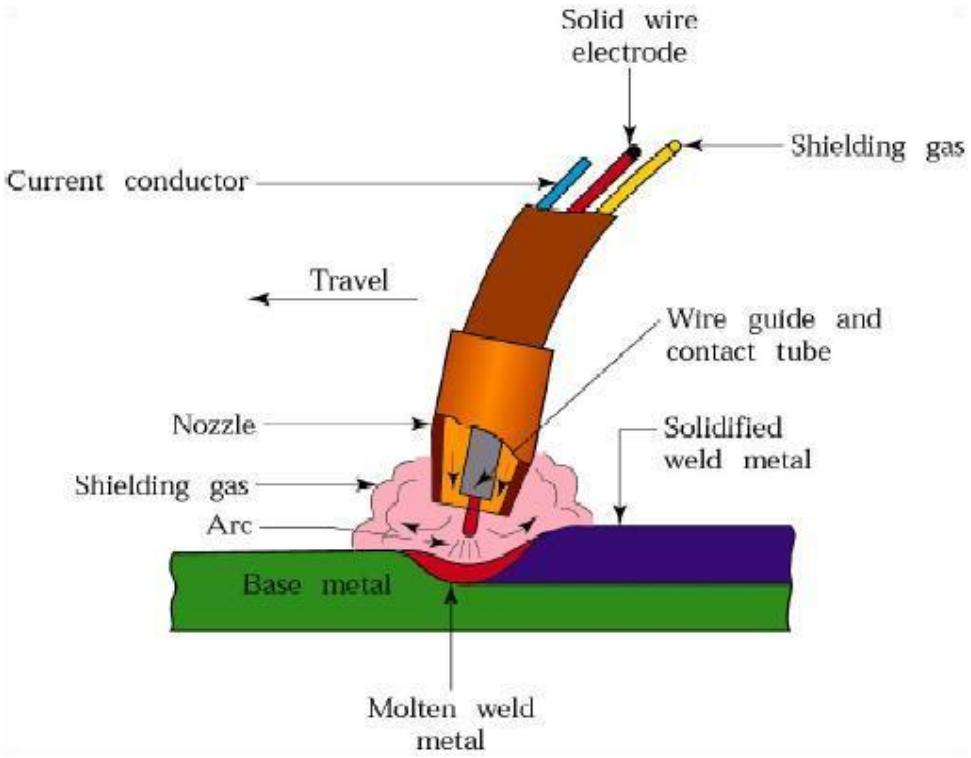

Figure 1.1: Principle of gas welding [http://www.weld….]

1.4 Equipment of MIG welding

Equipment of MIG welding consists of welding power source and cable, wire feed unit comprises of electric motor and pair of driving rolls etc. welding torch or wire electrode coiled on spool, Shielding gas cylinder with flow meter and pressure regulator and control of current, inert gas and electrode wire.

1.4.1 Power Sources

The majorly used power sources are AC transformer with rectifier or DC generator. Direct current electrode positive polarity that is electrode is connected to positive terminal and workpiece is connected to negative terminal is generally used because it provide more heat on electrode, deeper penetration and arc cleaning action. Direct current electrode negative polarity is used where we need to weld thin sheets or less penetration is required. AC is rarely used because burns off rates are unequal during positive and negative half cycles of AC.

1.4.2 Welding Gun

Welding gun is an important part of MIG welding. Welding gun feeds the electrode, shielding gas and also energises the electrode. Welding gun can be air cooled or water cooled, depending on heat generated. Generally water cooling is used when working current is above 250 A. The gun must be easy to handle, light weight and able to weld complicated shapes.

1.4.3 Wire Feed Mechanism

Wire feed mechanism have an important role in MIG welding. Wire feed mechanism feed the wire to the welding gun from a wire spool mounted on machine through rollers. Rollers are powered by wire feed motors which are able to push electrode wire to several yards. Wire feed unit is able to feed electrode at constant or variable speed. Electrode wires of different diameter can be feed through wire feed unit. Wires become difficult to handle as their diameter decreases.

1.4.4 Shielding Gas Cylinder

Shielding gas cylinder, pressure regulator and flow meter are essential equipment of metal inert gas welding. Shielding gas is supplied to nozzle through a hose pipe. Pressure regulator is to regulate the gas pressure and flow meter indicates the gas flow rate of the gas.

1.5 Effect of Welding Parameter on MIG welding

MIG can provide good quality of welds according to requirement of a job. MIG is able to weld both thick and thin type of workpiece at high speed and produce neat welds. For getting desired properties in weld we need to choose appropriate parameters. These parameters are discussed below.

1.5.1 Welding Current

Welding current is an important parameter in MIG welding. Amount of welding current decides the mode of metal transfer during welding. Increase in current leads to increase in melting rate of electrode and promote spray mode of metal transfer. Penetration of weld increases with increase in the welding current. Welding current must be chosen according to the thickness of workpiece and welding speed.

1.5.2 Voltage

Welding voltage is another important parameter in MIG welding. Welding voltage depends on arc length. Increase in arc length leads to increase in welding voltage which results in wider weld bead. If welding voltage too high it results in undercut. Welding voltage is also affects the mode of metal transfer. At low voltage globular and short circuit mode of metal transfer occur, whereas at high voltage spray mode of mode of metal transfer occur.

1.5.3 Diameter of Wire Electrode

Diameter of wire plays an important role in MIG welding. Diameter of wire affects the mode of metal transfer. For the same amount of current thinner wire produce more droplets of metal than the thicker wire of same material. Wire with less diameter results in deep penetration and high deposition.

1.5.4 Gas Flow Rate

Gas flow rate is an important parameter in MIG welding. Flow rate must be sufficient so that it can envelope the complete weld pool, heat affected zone, base metal and electrode from the atmosphere. Higher gas flow rate cause turbulence in the weld pool and can result in defects in weld bead. On the hand lower value of gas flow rate result in improper shielding of weld pool so an optimum must be selected for MIG welding.

1.5.5 Welding Speed

Welding speed is an important parameter in the MIG welding. Welding speed affects the heat input. Increase in welding speed leads to lower heat input which results in shallow penetration and increase in width of weld bead. Low welding speed results in deeper penetration and narrower weld bead.

1.5.6 Electrode Stick-out

Electrode stick-out is an important parameter for controlling bead geometry, penetration and deposition rate. Increase in stick-out leads to increase in resistance which results in preheating of electrode. With preheating electrode melt at lower current and provide high deposition and shallow penetration. Very small stick-out may result in damage to cotact tube. Generally stick-out is kept 10-15 mm.

1.5.7 Shielding Gas

Shielding gases play an important role in MIG welding. Shielding gases shield the weld pool and electrode end from the atmospheric contamination. Shielding gas must be selected of suitable composition and level of purity. Shielding gases affects the penetration, burn off rate and mode of metal transfer. Shielding gas can be used as pure gas or mixture of gases. Properties of different shielding gases are discussed below

- **Argon: -** Argon is inert gas which get ionised easily and hence provide easy arc initiation. Heat conductivity of argon is low which results in lower arc voltage and lower heat input. Low heat input in argon shield result in defects like porosity and lack of fusion. For increasing stability of arc mixture of argon with oxygen is used.

- **Helium: -** Helium is an inert gas, which is difficult to ionise so arc initiation is also difficult then argon. Thermal conductivity and arc voltage of helium is very higher than argon which results in high heat input. Deeper and wider penetration is obtained by helium than argon. Risk of defects like porosity, hot cracking and under cut is less with helium. High flow rate of helium is required for efficient shielding because of its low density.

- **Carbon dioxide: -** Carbon dioxide is an active gas which can react with molten metal or filler metal. Carbon dioxide forms slag by reacting with alloying materials like silicon and magnesium in weld pool or weld surface. This slag formation reduces the amount of alloying element but it can be compensated by highly alloyed filler metal. High voltage is needed to dissociate the molecule of carbon dioxide. High thermal conductivity of carbon dioxide results in deep penetration and wide weld bead.

- **Oxygen: -** Oxygen is an active gas which reacts with metal and form oxides which are undesirable. However, some time addition of oxygen is needed to stabilise the arc. Oxygen is usually added in small amount. Addition of oxygen in arc reduces the surface energy in liquid droplets, which increases the fluidity in weld pool and good appearing weld.

- **Nitrogen: -** Nitrogen can be used as shielding gas in duplex stainless steel and austenitic stainless steel. For steels maximum 5% of nitrogen can be added in other shielding gases. For welding of copper 100% nitrogen can be used as shielding gas. Nitrogen leads to formation of nitrides in unalloyed steels which is undesirable. However in nitrogen alloyed austenitic steel it is favourable as it compensate for nitrogen loss from weld pool.

- **Hydrogen: -** Hydrogen is an active flammable gas. Hydrogen is used in small amounts in a mixture with argon. Hydrogen is generally used in welding of austenitic steel and nickel alloys. High voltage is required for arc initiation in hydrogen atmosphere which leads to high heat input. Hydrogen reduces the oxides and results in cleaner weld. However high amount of hydrogen leads to porosity.

1.6 Advantages of MIG Welding

MIG welding is used extensively in wide range of industries because of its many advantages and suitability of weld both ferrous and non-ferrous materials.some of advantages of MIG welding are discussed below.

- MIG welding is faster than tungsten arc welding and manual metal arc welding because of electrode is fed continuously which makes it suitable for industrial application.
- MIG is suitable for welding of both thick and thin type of workpiece efficiently
- MIG welding is able to achieve deeper penetrations and high deposition rates
- MIG welding is flexible to automation according to the need of industry.
- There is no need of flux in MIG welding.
- MIG welding provides smooth, clean and spatter free weld bead. There is no need of post cleaning of weld.

- Higher travel speed in MIG weld results in considerable reduction in distortion.
- Amount of fumes generated in MIG is less than flux cored arc welding and shielded metal arc welding.

1.7 Disadvantages of MIG Welding

There are some disadvantages of MIG welding which are discussed below.

- Equipment of MIG welding is complex and costly. Portability of MIG welding is also less.
- Cooling rates of weld metal are higher than other slag forming processes.
- For outdoor application MIG welding is not suitable as air drafts may disturb the shielding gas envelope.

1.8 Applications of MIG Welding

- MIG welding can be used to welding wide range of ferrous and non-ferrous materials like carbon and low alloy steels, stainless steels, magnesium, nickel, aluminium and their alloys etc.
- MIG welding can be used for the welding of die steel and tool steels.
- MIG welding is used in many industries like refrigeration industry, automobiles, air crafts, ship building and pressure vessel manufacturing etc.

1.9 Stainless Steel

Stainless steels are steels which are having minimum 11.5 % chromium in them. Affinity for oxygen is higher in chromium than iron, this leads to formation of chromium oxide layer on the surface. This layer protects the steel from any reaction with the surrounding atmosphere and imparts corrosion resistance and oxidation reduction. In stainless steel, alloying elements other than chromium are also added like nickel, manganese and molybdenum. Stainless steel can be classified in following categories [Folkhard, 1988].

- Ferritic stainless steel
- Martensitic stainless steel
- Austenitic stainless steel
- Duplex stainless steel
- Precipitation hardenable steel

1.9.1 Ferritic Stainless Steel

These are stainless steels having chromium content from 11.57 to 27% and carbon content from 0.08 to 0.2%. Low carbon content provides reduced sensitization and improves toughness. Yield strength of these steels is 275-415 MPa and tensile strength is between 500-600 MPa. These steels are cheaper than austenitic stainless steel and become popular in domestic and catering atmospheres such as sinks, washing machines, drainers etc. ferritic steels having good machinability, lower thermal expansion and higher conductivity than austenitic steel. Common grades of ferritic steels are AISI 405, 409, 430, 444 etc.

1.9.2 Martensitic Stainless Steel

Martensitic steels are having chromium content 12-17% and content of carbon lie between 0.1 to 1.20%. Yield strength of 150-1860 MPa can be achieved by hardening and tempering of martensitic steel. Hardenability of these steels increase with increase in chromium content. Common grades of martensitic steels are AISI 403, 410, 414, 440 etc. these steels are hard and brittle.

1.9.3 Austenitic Stainless Steel

Austenitic stainless are having chromium content of 16-25% and ample amount of austenite stabilizers like nickel, manganese and nitrogen to stabilize the austenitic phase at the room temperature. Nickel is main austenitic stabilizer in AISI 300 series, generally content of nickel lies between 8-20%. In AISI 200 series nickel is partially replaced by cheaper manganese. Austenitic steels are having FCC structure, non-magnetic in nature, show good ductility of about 50% and good toughness at low temperatures. Common grades of austenitic stainless steel are AISI 304, 316, 302, 310, 210 etc.

1.9.4 Duplex Stainless Steel

Duplex stainless steels have both ferrite and austenitic phase in microstructure. In duplex steel properties of both austenitic and ferrite steel are their like weldability and toughness of austenite and localized corrosion resistance of ferrite. Corrosion resistance and strength of duplex steels are higher than simple austenitic stainless steel. Common grades of duplex steel are SAF 2205, ferralium, 225 DP-3 etc.

1.9.5 Precipitation-Hardenable Steel

Precipitation-hardenable steels are having attractive combination of properties of both austenitic and martensitic grade. These steels are having good tensile strength and resistance to corrosion. Tensile strength came from precipitation hardening of austenitic or martensitic matrix after the heat treatment. Content of carbon kept low in these steels because carbon does not take part in precipitation. Application of these steels is mainly in aerospace industry.

1.10 Effect of Alloying Elements on Stainless Steels

Stainless steel consists of number of alloying element. These alloying elements are added to get desired properties in stainless. Different alloying elements have their different effects on the steel. Effect of some alloying elements is discussed below.

1.10.1 Carbon

Carbon is added iron to increase its hardness and strength. Hardening and strengthening of steel after heat treatment is because of addition of carbon. In ferritic, austenitic and duplex stainless steels content of carbon (0.005 to .03 %) is kept low to prevent carbide precipitation.

1.10.2 Manganese

Manganese is an austenite stabilizer. Manganese increases hardenability, toughness, strength and hot working properties. In AISI 200 series of austenitic steel manganese is used as substitute to nickel, for stabilization of austenite.

1.10.3 Chromium

Chromium is added in high amount in the stainless steels. Chromium provides the resistance against oxidation by forming a layer of chromium oxide. This self-repairing layer of chromium oxide prevents stainless steel from corrosion. Minimum chromium content in stainless steel is above 11.5 %. Corrosion resistance increases with increase in chromium content.

1.10.4 Nickel

Nickel is stabilizer of austenite which provides good toughness and strength at low and high temperatures. Nickel also improves resistance to corrosion.

1.10.5 Molybdenum

Molybdenum increases the resistance to pitting and crevice corrosion in stainless steels. It improves strength and hardness at high temperatures.

1.10.6 Nitrogen

Nitrogen is an austenite stabilizer and it is cheaper than nickel. As an austenite stabilizer addition of nitrogen improves yield strength.

1.10.7 Titanium

Titanium is added to prevent precipitation of chromium carbide. Precipitation of chromium causes decrease in corrosion resistance. Addition of titanium results in formation of titanium carbide which is stable and not easy to dissolve in steel.

1.11 AISI SS 304

AISI 304 is grade of austenitic stainless steel. AISI SS 304 is also popular with name 18/8. Name 18/8 is derived from its nominal composition that is 18% chromium and 8% nickel. SS304 is widely used stainless steel. Tensile strength of SS 304 is about 520-720 MPa. SS 304 shows strong resistance to oxidation and corrosion. SS304 shows good weldability either with or without fillers. Hardening of SS 304 cannot be done by heat treatment. SS 304 is wide range of applications like sinks and splash backs, cutlery and flatware, tubs, saucepans, springs, nuts, bolts, equipment in industries like dairy, brewery, food and pharmaceuticals.

1.12 Organization of Thesis

The thesis report is divided into five chapters. Chapter one gives introduction about metal inert gas welding, its equipment, advantage and disadvantage, this chapter also gives introduction about stainless steel. Chapter two gives review of literature on welding of austenitic stainless steel. Chapter three gives description of design of experiment, pilot study and methodology used during this study. Chapter four contains result and discussion of the experiments done during this study. Chapter five includes conclusion of this study and future scope for this study.

Chapter 2

Literature Review

2.1 Introduction

This chapter deals with review of literature on metal inert gas welding of austenitic stainless steel. This chapter gives information about the research that have been done in this area and on which topics currently research is going on. Findings of different researchers related to metal inert gas welding is discussed in this chapter. This chapter also includes literature summary and scope and objective of present study.

2.2 Literature Review

Murugan and Parmar [1994] studied the effect of MIG welding parameter on weld bead geometry and dilution percentage. 20 mm thick plates of structural material IS 2062 is welded by AISI 316L stainless steel wire. Four parameters (open circuit voltage, feed rate, welding speed and nozzle to plate distance) were taken into consideration in this study. Argon is used as shielding gas at pressure 20 L/min. A five level factorial model was developed to predict the weld bead geometry. Penetration was found to be unaffected at voltage 30-31 V irrespective of other parameters. Voltage was found to have maximum effect on width of bead. Dilution was found to be significantly reduced when nozzle to plate distance was increased.

Tusek and Suban [2000] studied the effect of addition of hydrogen in the shielding gas in MIG and TIG welding of austenitic stainless steels. Base metal of thickness 8 mm and 10 mm was welded in TIG and MIG respectively. Current was varied at three levels that is 100, 150 and 250 A. Amount of hydrogen in argon shielding gas is varied at five levels that is Ar+0.5% H_2, Ar+1%H_2, Ar+5%H_2, Ar+10%H_2, and Ar+20%H_2. Five samples were prepared at each level of current with different shielding gas. Arc resistance and arc energy increased with addition of hydrogen in shielding gas. Melting efficiency in case of TIG was found to be increased with increase in current and hydrogen addition. Melting efficiency is found to be increased by 30 to 50% with addition of hydrogen in the argon shielding gas.

Murugan et al. [2001] studied the residual stresses due to multipass welding of AISI

304 stainless steel and low carbon steel. Plates of different thickness (6, 8 and 12 mm) of both the materials were taken for study of residual stresses for each pass. For the measurement of residual stresses X-ray diffraction method was used. A peak temperature in stainless steel was higher in low carbon steel even at low temperature because of lower thermal conductivity of stainless steels. With increasing number of passes residual stress found to be decreasing in the root side whereas increasing on the top side.

Gulenc et al. [2005] studied the effect of hydrogen in shielding gas during MIG welding of austenitic stainless steel. AISI 304L plates of 140 x 75 x 10 mm were welded by MIG welding and their mechanical and microstructural properties were studied. Welding was done in three shielding environment by varying the amount of hydrogen (pure argon, argon + 1.5 % H_2 and argon + H_2) in argon. Current was varied at three levels (140, 180, 240 A). Best tensile strength of weld sample was found at the 240 A current and argon + 1.5% H_2. Best value of toughness was found at 240 A current and argon + 5% H_2. Toughness increased with increase in amount of hydrogen in shielding gas. Hardness value of base metal was found to be higher than heat affected zone.

Furusawa and Yasuda [2009] investigated the gas metal arc welding (GMAW) conditions and procedures for an efficient stainless steel welding procedures. AISI 304 plates of thickness 2-9 mm were used as testing specimen and Y308 of 1.2mm diameter was used as welding wire. Ar + 3% O2 mixture was used as shielding gas for metal inert gas welding (MIG) welding and CO_2 shielding gas was used for flux cored wire metal active gas (MAG) welding. Wire extension was kept constant at 15mm and 20 mm for MIG and MAG respectively. A reference voltage (E_T) was selected, as no shot circuit at this voltage or above it. Significant increase in penetration was found above transition current (170 A), at voltage E_T + 2 V. when welding was done at voltage E_T – 2 V that is at short arc stable arc was found with not much change in penetration with change in welding current. A continuous satisfactory bead was formed when welding was done at voltage E_T – 2 V, but at voltage E_T and E_T+2 V discontinuous bead was formed for current 100 A, 150 A and 200 A. insufficient penetration was observed in horizontal fillet welds of 3 mm thick plates at lower welding currents, however sufficient penetration was obtained for same workpiece using pulsed MIG welding. Pulse duration of 1 msec was used with 330 A as average pulse current. For I butt welding, quantity of the metal deposited per unit weld length Vw mm^3/mm must be two times of root opening for good penetration. For MAG satisfactory results were found at approximately 2 V above the E_T.

Giridharan and Murugan [2009] developed a mathematical model that correlates controllable input parameters of pulsed gas tungsten arc welding (GTAW) like welding speed, pulse current and pulse duration with weld bead parameters like bead width, penetration aspect ratio. Design of experiment (DOE) used for development of model was based on central composite rotatable design. Sheets of AISI 304L of dimensions 100x50x30 mm were welded by pulsed TIG process, without any edge preparation. Pure argon was used for shielding and commercial grade argon was used for back purging. Welding speed, pulse current and pulse current duration were varied at 5 levels and other parameters like pulse frequency, arc length, gas flow rate and mean arc voltage were kept constant. Bead parameters i.e. depth of penetration, width of bead and aspect ratio were measured by digital planimeter and optical profile projector. Regression modelling was used to weld bead geometry. Values predicted had shown agreement with experimental values. Welding speed was found to be most significant factor followed by pulse current and current duration on bead parameters. Interactions of pulsed current and welding speed were found significant on bead area.

Aghakhani et al. [2011] studied the effect of welding parameters like wire feed rate, welding voltage, nozzle to plate distance , welding speed and flow rate on the weld dilution. A mathematical model by Taguchi's method was developed. Experimentation was done on plate of dimensions 200 x 100 x 6 mm with consumable electrode of diameter 0.8 mm. wire feed rate was found have most significant effect on the weld dilution percentage. Voltage and nozzle to plate distance was also found as significant parameter. Gas flow rate was found to have less significant for the weld dilution.

Galvis and Hormaza [2011] observed different failure mode of SS 304 weld joints prepared by different welding processes. Welds were prepared using SMAW, FCAW and GMAW using type 308 stainless steel filler electrode. Welding was done in three passes for all the welding processes. Heat input in all the processes was nearly equal i.e. 0.77 kJ/mm. Fractograph analysis showed globular oxides of small size were present in welds. Mean grain size of HAZ was found to be different for different welding processes. Two types of morphologies (lathy and skeletal) of ferrites were found. Stress concentrator at weld root was first mode of failure this is because of change in cross section area at weld root; crack propagates through HAZ or weld. Second mode of failure was at HAZ because of variation in grain size. Third mode of failure is due to inclusions of oxides or slag, which worked as stress raiser. Welds prepared by FCAW showed best fatigue properties.

Kumar et al. [2011] studied the effect of process parameters of submerged arc welding like welding current, arc voltage, flux composition, and travel speed on the changes in microstructure and microhardness of the heat-affected zone (HAZ). Process was optimized to minimise the changes occur in the material properties after submerged arc welding process. Changes in the microstructure and resultant changes in ferrite percentage, bainite, pearlite, and martensite formations were studied by micrographs of weld metal. Most significant factors for changes in metallurgical properties and microhardness were found to be welding current and type of flux. When welding current was increased from 350 to 450 Amp, microhardness increased significantly. Flux with higher basicity index of 1.6 exhibited lower microhardness than flux with lower basicity index of 0.8. Lowering of microhardness in flux of basicity index 1.6; it is due to higher amount of MgO and CaO, has tendency to pick up the carbon from steel, thus lowering the microhardness.

Kumar and Shahi [2011] studied the effect of heat input on the microstructure and mechanical properties of AISI 304 stainless steel during gas tungsten arc welding. AISI 304 plates of dimensions 200 x 100 x 6 mm were welded with AISI 308 filler wire of diameter 3.15 mm. Joint was prepared with two number of passes with interpass temperature of 150 degree Celsius. Voltage is varied at three levels (30, 35, 40 V). All the joints showed a good tensile strength. Maximum tensile strength and ductility was found in the welds which are welded at low heat input. Dendrite size is found to be increased with increasing heat input. Size of HAZ and fusion zone was increased with increasing heat input. Coarse grains were found in HAZ of all the welds, with increase in heat input grain become coarser. Author recommended low heat input for welding of austenitic stainless steels.

Kyriakongonas et al. [2011] investigated the multipass welding of austenitic stainless steel. Two set of SS 316L plates were welded having dimensions 350 mm x 150 mm x 8 mm and 700 mm x 300 mm x 8 mm by a robotic welding arm. Flux cored arc welding was done in this experiment with a shielding gas mixture of 82% Ar and 18% CO_2. Welding was done in three passes by keeping current, voltage, welding speed, and gas flow rate constant. In this study thermal cycle, deformation and residual stresses in welded specimen were measured, in addition metallurgical study and finite element modelling (FEM) was done to predict the thermomechanical response of weld joint. It was found that microhardness of fusion zone was higher than HAZ results of thermal and residual stresses matched with values predicted by model.

Srinivasan and Balasubramanian [2011] investigated the influence of heat input on

generation of fumes and their composition during GMAW of austenitic stainless steel AISI 316. 5 mm thick plate of AISI 316 stainless steel was welded with AWS ER308L as filler wire of diameter 1.2mm. Argon was used as shielding gas at a flow rate of 10 L/min. Welding current was varied at 5 levels that is 90, 110, 130, 150 and 170 A with welding voltage between 20-23 V. Wire feed rate varied at five levels that is 3.13, 4.62, 5.61, 7.09 and 8.14 m/min. Heat input was varied at 5 levels 0.96, 1.03, 1.15, 1.26 and 1.32 kJ/mm. Heat input of 1.15 kJ/mm was found to be best for enhancing ultimate tensile strength, yield strength impact toughness and joint efficiency. Acicular delta ferrite in austenite increases tensile strength and impact toughness. Increase in heat input results in vermicular and lathy delta ferrite, which reduces impact toughness and tensile strength. Microhardness increases with increasing heat input and further decrease with increasing heat input.

Kumar et al. [2012] studied analysis of TIG and MIG on austenitic SS with dye penetration testing. Voltage was taken constant and various characteristics such as strength, hardness, ductility, grain structure, modulus of elasticity, tensile strength breaking point, HAZ are observed in two processes and analysed and finally concluded. A sample of SS 304 of dimensions 150 x 50 x 3 mm was taken and both welding are done. From the results it was found that TIG is better than MIG. The quality characteristics parameters are ultimate tensile strength, ultimate load, and percentage elongation. Porosity and intergranular corrosion was also observed with the help of metallurgical study.

Niagaj [2013] discussed the different methods of welding stainless and ways by which effectiveness and productivity of these methods can be enhanced. New variants of different welding methods along with implementation of modern welding equipment and application of special welding consumables were discussed. Different welding methods discussed were tungsten inert gas (TIG) welding, metal inert gas/metal active gas (MIG/MAG), manual metal arc (MMA), plasma arc welding (PAW), submerged arc welding (SAW), flux cored arc welding (FCAW) and laser beam welding (LBW). Implementation of mechanization/automation and use of new variations of MIG can improve its productivity. Better results were obtained, when welding is done with Ar with 2-3% of CO_2 rather than pure argon. In MAG mixture of gases like hydrogen and/or helium, along with Ar+CO_2, results in increase in depth of penetration, improved welding speeds and smoother weld surface.

Nanda et al. [2013] studied the mechanical properties of gas metal arc welded austenitic stainless steel SS304. Welding current was varied at three levels (180 A, 280 A and

350A) and welding wire speed was varied at three levels (2 m/min, 3 m/min and 5 m/min). Voltage was kept constant at 24 V. CO_2 was used as shielding gas at constant pressure of 3kg/cm^2. Maximum tensile strength was found at 250 A current and at wire speed of 3 m/min. Microhardness of HAZ and weld metal was found maximum at 250 A current and wire speed 3m/min.

Sathiya et al. [2013] studied Genetic algorithm based optimization of the process parameters for gas metal arc welding of AISI 904L stainless steel. Box behnkan technique was used to design the parameter. The input parameters like gas flow rate, voltage, travel speed, wire feed speed were taken under consideration. Effect of input parameters were studied on bead width, bead height and depth of penetration with the help of optical microscopy. The mathematical model was developed by regression analysis. Genetic algorithm was used to minimize bead width, height. Genetic algorithm was used to optimize the solution. It was found that genetic algorithm provide solution much faster and accurate as compare to regression analysis. Confirmation tests were carried out and error less than 2% was found.

Yilmaz and Tumer [2013] investigated the impact toughness and microstructure of dissimilar welds of austenitic stainless steel 316L and Low alloy steel AH36. Plates of dimension 450 mm x 150 mm x 14 mm were welded by flux cored arc welding using E309LT1 filler metal. Four different shielding gas mixtures (Ar + 12% CO_2, Ar + 20% CO_2, Ar + 50% CO_2, and 100% CO2) were used during the experiment. Interpass temperature was kept constant at 150˚C. Impact test for notched specimen were done at-40˚C,-20˚C, 0˚C and 20˚C temperature. Microhardness of specimens was measured at base metal, weld metal and transition zone under 200g of load. Increase in amount of CO_2 increased the melting rate of base metal and filler metal. Amount of CO_2 also affected the morphology and amount of the delta ferrite. Increase in amount of CO_2 results in reduced amount of delta ferrite and increased the amount of austenite. Microhardness was found to be decreased with increase in amount of CO_2 in shielding gas. Energy dispersive spectroscopy (EDS) showed inclusions composed of multiple complex oxides, with increase in amount of CO_2 size of and amount of inclusions were found to be increased. Impact toughness was found to be decreased with increased amount of CO_2 in shielding gas due to increased amount of inclusions.

Bhattacharya et al. [2014] studied the effect of heat input on penetration while welding AISI 304 plates by automatic gas metal arc welding. A bond graph model for fusion zone and depth of penetration was developed and validated experimentally. Plates of

dimension 100 x 50 x 6 mm were welded by automatic gas metal arc welding by varying current, voltage, welding speed and gas flow rate at different levels. Levels of each parameter were as: voltage 20, 22, 22 V; current 140,160,180 A; gas flow rate 8, 12, 16 L/min and welding speed 2.5, 4, 6 mm/s. To study the effect of these parameters on toughness taguchi L9 orthogonal array was applied for experimentation. Microstructural study of specimens was done by scanning electron microscopy. Bond graph approach was found to be better and time saving alternative for prediction of depth of penetration, fusion zone profile and temperature. Increase in heat input resulted in increase in fusion zone and penetration. Increase in voltage resulted in increase in toughness and fusion zone.

Chauhan and Jadaoun [2014] studied the MIG welding of SS 304 and low carbon steel. In the study three parameters that is current, voltage and welding speed was taken into consideration. Current (80, 100 and 120 A), voltage (16, 19, 22 V) and welding speed (30, 40 and 50 cm/min) were varied at three levels. Gas flow rate was taken 9 L/min. Taguchi method was used to find the influence of parameters. Voltage and welding speed was found to significantly affect the ultimate tensile strength.

Vasantharaja et al. [2014] studied the distortion and residual stresses on 316LN stainless steel plates welded by TIG and activated TIG. Austenitic stainless steel plates of thickness 16mm were welded using SS 316L filler wire of 1.6 mm diameter. Three types of joints were prepared i.e. square butt joint, double V groove joint and Y groove joints, with including edge angle of 70˚ in grooved joints. Distortion was measured by using height gauge. Microstructural examination was done by optical microscope. Residual stresses in the weldments were measured by ultrasonic technique by using L_{CR} waves. Radiography of all samples was done for detection of defects. Double sided activated TIG weld had lower tensile residual stresses, lower amount of ferrite and coarse grain size. Size of grain in TIG welds was smaller with high amount of ferrite and high tensile residual stress value, because of higher volume of weld metal due to V groove preparation. Double sided TIG and activated TIG welds showed lower distortion than Y groove joint because of distribution of residual stresses was non uniform on top and bottom side of joint. Author recommends double-sided activated TIG welding for minimum distortion and residual stresses in welds.

Kumar and Shahi [2014] studied the effects of welding on the mechanical properties and microstructure of austenitic stainless steel. AISI 304 stainless steel plates of dimension 300 x 100 x 6 mm were welded by AISI 308 filler wire of 1.6 mm and 2.4 mm for root pass and main pass respectively. Welding was done in three passes; root pass was welded in all the

samples by 100 A current and 11 V of voltage. For middle and cover pass current (120, 150 and 180 A) and voltage (13, 15, 18 V) were varied at three different levels. Welds prepared at low heat input showed maximum tensile strength and ductility. Weld zone and HAZ welded at low heat input showed better impact toughness than welds which are prepared at high heat input. HAZ showed grain coarsening which was found to be increased with increasing heat input.

Kumar et al. [2014] studied mechanical and metallurgical properties of two dissimilar stainless steels i.e. duplex 2205 and AISI 316. Effect of double layer shielding along with five other parameters i.e. current, filler material, voltage, gas flow rate and type of shielding gas were studied. Taguchi L27 orthogonal array was used for designing experimental conditions. Influences of input parameters on tensile strength, microhardness and microstructure of weld were observed. Microhardness and tensile strength were improved by using double layer shielding effect with respect to single layer shielding. Voltage, filler material and type of shielding gas significantly affected the tensile strength. Microhardness and tensile strength were increased with increase in current and voltage but at very high values it reduces joint strength.

Mirshekari et al. [2014] studied the effect of single pass, double pass and triple pass TIG welding on the corrosion behaviour, microstructure and hardness of AISI 304L austenitic stainless steel. Plates of AISI 304L of dimension of 200 x 100 x 6 mm were welded by AISI 308 wire of 2.4 mm diameter as filler wire. The hardness value was found to be increased with increase in number of passes. Potentiodynamic polarization curves and immersion tests showed that corrosion resistance increased with increase in number of passes. Weld with three passes found to have highest corrosion resistance.

Gouveia et al. [2014] studied the effect of interpass temperature on impact toughness; microstructure and fatigue crack propagation plates of soft martensitic stainless steel CA6NM of dimensions 110 mm x 35 mm x 20 mm were welded by TIG welding. Welding input parameters like voltage, current, welding speed, gas flow rate were kept constant except interpass temperature. Interpass temperature was varied at two levels i.e. 80˚C and 150˚C. welds were free from porosity and cracks. Interpass temperature influenced the formation of delta ferrite; with 80˚C interpass temperature delta ferrite was formed at intergranular locations whereas with 150˚C delta ferrite formed between Widmanstatten plates. Influence of interpass temperature was not significant on microhardness of weld zone and HAZ. Impact toughness was found to be increased at 80˚C interpass temperature. Rate of crack growth was

found to be reduced at lower interpass temperature than higher interpass temperature.

Saha et al. [2015] investigated the texture, microstructure and mechanical properties of GMAW welded SS 304. Sheets of SS 304 of dimension 200 mm x 70 mm x 4 mm were welded by using SS 316L as filler metal. Welding was done at two conditions by varying current, welding speed and wire feed rate however heat input and gas flow rate were kept constant. Influence of welding parameters was studied on microstructural constituents by using transmission electron microscope (TEM). Electron back scattered diffraction (EBSD) was used to observe micro texture evolution, grain boundaries, orientation data and disorientation distribution. Mechanical properties like tensile strength and hardness were also investigated. It was found that welding speed and current has significant effect on percentage dilution which results in change in morphology of delta ferrite. Coarse grain structure was found at HAZ and due to carbide precipitation dark narrow sensitized zone formed near fusion boundaries. Fusion zone showed higher hardness than heat affected zone and base metal. Author recommends high current with high welding speed for enhancing mechanical properties.

Tathgir and Bhattacharya [2015] investigated the effect of different fluxes, shielding gas composition and current on the TIG welded low alloy steel, duplex stainless steel and austenitic stainless steel. Plates of dimension 100 mm x 50 mm x 5mm were welded using 14 fluxes i.e. MoO_3, TiO_2, MoS_2, SiO_2, MnO_2, NiO, ZnO, Al_2O_3, CrO_3, $CaCO_3$, NaF, CaF_2, KCl and KBr. Voltage, torch angle and speed of welding were kept constant. Three shielding gas compositions (i.e. pure argon, 95% Ar + 5% H_2 and 70% Ar + 30% He) were used during this study. SiO_2, MoS_2, MoO_3, TiO_2 and CrO_3 fluxes showed significant increase in depth of penetration with respect to other fluxes for all the steels. Addition of H_2 and He in shielding gas increased the depth of penetration because of increased heat conduction and melting efficiency. Effect of H_2 is more on depth of penetration than He. Among all other steels austenitic stainless steel showed more increase in depth of penetration.

2.3 Literature Summary

Survey of literature has showed that austenitic stainless steel has vast industrial and domestic applications. These applications lead to study of the welding processes of austenitic stainless steels. Researchers had done investigation in various fields of welding of austenitic stainless steels. Some researchers developed model to understand the distribution of heat and distribution of stresses during the welding process. Models are also developed to optimise the

welding parameters by techniques like finite element modelling (FEM), bond graph modelling, quasi-newton numerical optimisation, Box behnkan and regression analysis [Bhattacharya et al., 2014; Aghakhani et al., 2011; Giridharan and Murugan, 2009; Kyriakongonas et al., 2011]. Some researcher investigated bead geometry parameters (depth of penetration, bead width, bead height etc.) and effect of welding input parameters (voltage, current, gas flow rate, welding speed etc.) on it [Murugan et al., 2001; Giridharan and Murugan, 2009; Tusek and Suban, 2000; Bhattacharya et al., 2014]. Some of the researchers studied the influence of change in composition of shielding gas [Tusek and Suban, 2000; Gulenc et al., 2005; Sathiya et al., 2013; Tathgir and Bhattacharya, 2015]. Some of researchers studied the effect of welding input parameter on mechanical properties like tensile strength, impact toughness, microhardness, fatigue strength and bending strength [Sathiya et al., 2013; Gulenc et al., 2005; Kyriakongonas et al., 2011; Bhattacharya et al., 2014; Galvis and Hormaza, 2011; Kumar and Shahi, 2011; Kumar and Shahi, 2014; Kumar et al., 2014]. Microstructure of weld was extensively studied by many researchers by optical microscopes, SEM, TEM, XRD etc. [Gulenc et al., 2005; Kyriakongonas et al., 2011; Bhattacharya et al., 2014; Galvis and Hormaza, 2011; Kumar and Shahi, 2011; Kumar and Shahi, 2014; Kumar et al., 2014]. Few authors studied thermal cycles, residual stresses and distortion in austenitic stainless steel welds [Kyriakongonas et al., 2011; Murugan et al., 2001; Vasantharaja et al., 2014]. Few researchers studied activated tungsten arc welding by applications of various fluxes during welding and studied their effect on weld geometry. [Vasantharaja et al. 2014; Tathgir and Bhattacharya, 2015].

2.4 Scope and Objective of the Present Study

Welding of austenitic stainless steel has large scope, because of its extensive applications, which are increasing day by day due to its high strength, weldability and corrosion resistance. Literature survey revealed lot of research work had been done in the area of welding of austenitic stainless steel. Many researchers are currently studying the various fields of welding of austenitic stainless steel. In case of MIG welding of austenitic stainless steel, there is still not very rich knowledge base available. This makes it important to research in the various fields welding of austenitic stainless steel, some of the fields that can be studied are discussed further. Modelling of welding using different techniques like FEM for better understanding of process and prediction of properties to minimise the experimental work in experimentation. Optimisation of MIG welding input parameters for enhancement of joint

performance. Use of different fluxes in MIG welding of austenitic stainless steel need to be study more to increase the efficiency of welding and develop knowledge base of activated MIG welding . Study of distribution of residual stress and distortion can be studied and the parameters responsible for it can be optimised.

Taking all above factors into consideration this present study is focussed on multipass metal inert gas welding of SS 304 grade of austenitic stainless steel. Objective is to study the

- Influence of various input parameters of MIG welding on impact toughness of SS 304 welds at room temperature and below room temperature.
- Influence of various input parameters of MIG welding on the distortion of SS 304 weld plates.
- Effect of different input parameters of MIG welding on microhardness of fusion zone and heat affected zone.
- Study the change in microstructure of fusion zone and heat affected zone.

Chapter 3

DESIGN OF EXPERIMENTAL STUDY

3.1 Introduction

This chapter deals with the details of the methods by which experimental work is done during this study. The objective of this work is to study the influence of MIG welding input parameters on austenitic stainless steel welds. During this study impact properties, distortion and microstructural changes during the multipass MIG welding in austenitic stainless steel were studied. This chapter contains the process that is taken during welding and testing in this study.

3.2 Material

In metal inert gas (MIG) welding two main materials are base metal and a filler metal. In MIG welding filler metal also serves the purpose of electrode.

3.2.1 Workpiece

This study is focused on properties of austenitic stainless steel welds. Common grades of austenitic stainless steel from AISI 300 series are AISI 304, 310, 316 and from 200 series are AISI 201, 202. AISI 304 is most widely used austenitic stainless steel because of its excellent corrosion resistance and weldability. AISI 304 is used as workpiece material. Plates of dimension 100 x 70 x 12 mm are used as work piece. Determination of chemical composition of base metal is done by foundry master atomic absorption spectrometer. This spectrometer works on worldwide analytical system (WAS) software. Composition of base metal is shown in table 3.1.

Table 3.1: Chemical composition of AISI 304

Carbon	Chromium	Nickel	Phosphorus	Manganese	Sulphur
0.0241	19.1	8.11	0.0392	1.47	0.005

3.2.2 Filler Material

In metal inert gas welding filler metal are generally of the similar composition of that base metal. In this study AISI 304 wire of 1.2 mm diameter is used as filler metal.

3.3 Equipment and Methodology

This section discusses about different equipment and methods used during this study. In this study experiments is done according to Taguchi orthogonal array. Flow chart of experimental plan is shown in figure 3.2.

3.3.1 Machine

A semiautomatic gas metal arc welding machine (Tornado MIG 350) available at Central workshop, Thapar University Patiala is used for welding of samples. Voltage adjusting range of this machine is 15 to 40 V and current adjusting range is 20 to 350 A. In this machine electrode diameter of 0.8, 1 and 2 mm can be used. Arc force can also be varied in this machine. Figure 3.1 shows the setup of machine. This setup is consist of transformer, wire feed unit, welding gun, argon gas cylinder and gas flow regulating valves. Gas flow rate is controlled by gas flow regulator and flow meter shows the value of gas flow rate. Argon gas cylinder is also part of this setup.

Figure 3.1: Set up of semi-automatic MIG machine

(**Courtesy:** Central Workshop, Thapar University, Patiala)

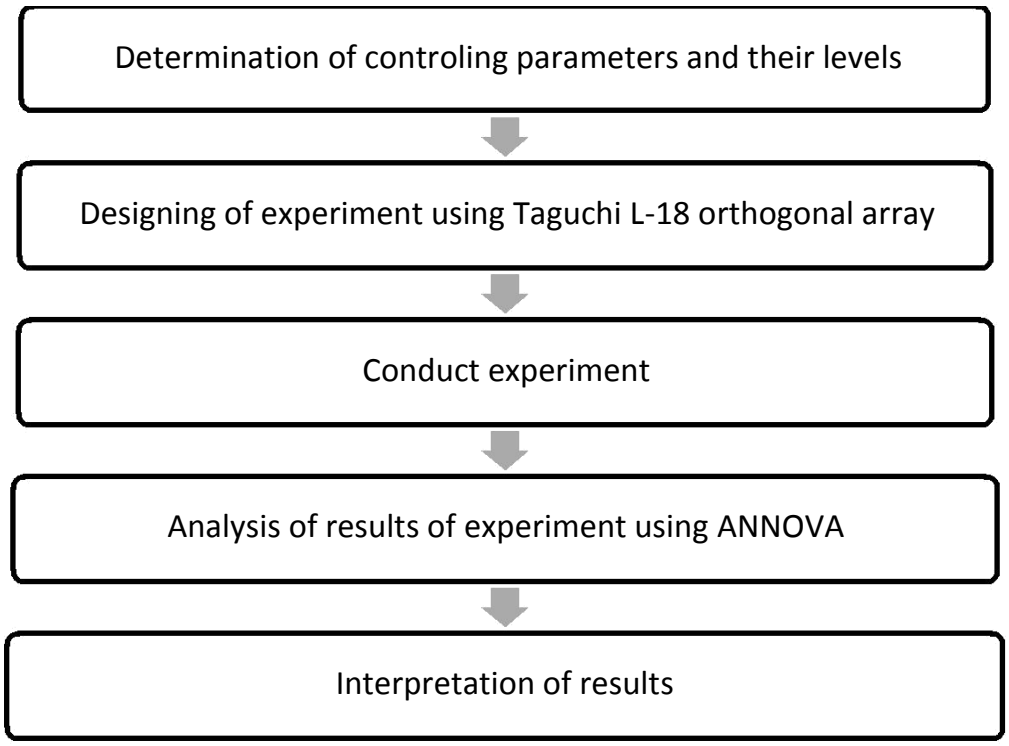

Figure 3.2: Experimental plan of study.

3.3.2 Pilot Experiment

In order to study the influence of current and voltage on the base material pilot study is done. In this pilot study layer of weld bead is deposited on the base metal by varying current and voltage at three levels (as shown in table 3.2) by keeping gas flow rate constant. Figure 3.4 shows the etched cut out specimen of plates welded at different values of current and voltage, below every bead value of current and voltage at which it is welded is mentioned. This study revealed that penetration of filler metal is very less with lower level of voltage (20 V) and current (150 A), so the lower level of current and voltage are not used in further study.

Table 3.2: Process parameters and their level for pilot study.

S.No.	Current (A)	Voltage (V)
1	180	22
2	180	24
3	210	20
4	210	22
5	150	20
6	150	22
7	150	24
8	180	20
9	210	24

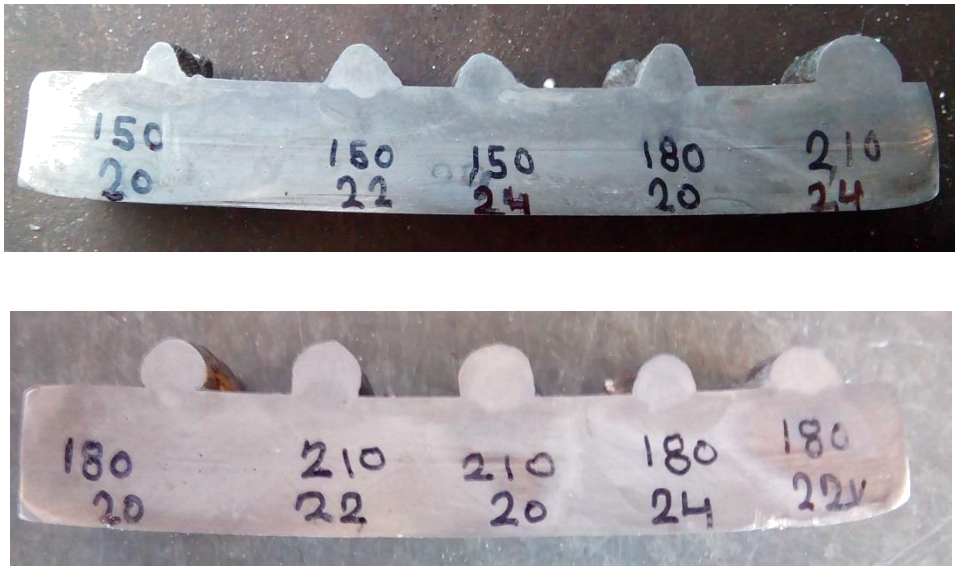

Figure 3.3: Etched specimens of plates welded for pilot study (upper value shows current and lower value shows value of voltage).

3.3.3 Orthogonal Array

The conventional method of investigating a large number of factors has been to analyze them one at a time. This is costly and an inefficient approach. Variables are grouped into the columns which form a matrix which is termed as an orthogonal array. Many factors and their interaction can be studied simultaneously by using orthogonal array. In normal experiments, the investigator alters the values of many variables. For determine how these variable should be altered, a suitable orthogonal arrays is generated by Dr. Genichi Taguchi by which the influence of all variables can be differentiated from each other. Selection of an appropriate orthogonal array is done on the basis of total degree of freedom of experiment. Degree of freedom signifies the number of comparisons to be made between the variables. The degree of freedom of a parameter is one less than the number of levels on which the parameter is varying. Degree of freedom of an interaction between two or more parameters can be calculated by multiplying the degree of freedom of the parameters those interacting parameters. Once degree of freedom of all the parameters is calculated next step is to select the appropriate orthogonal array. There are three types of orthogonal arrays i.e. 2 level (L4, L8, L16 etc.), 3 level (L9, L27 etc.) and mixed level (L8, L16, and L18 etc.). In this study Taguchi L18 orthogonal array is used for designing a set of experiment. L18 orthogonal array is a mixed level design having 8 columns and 18 rows. In L18 orthogonal array is a matrix with different set of parameters in every row, which results in 18 experiments. In L18

orthogonal array we can study eight parameters, one two level factor and a seven three level parameters.

3.3.4 Selection of Contributing Factor

In this study controlling factors are determined by pilot study and literature survey. Review of literature shows voltage, current, flow rate, edge including angle are important controlling factors which significantly affect the mechanical and microstructural properties of weld. Interpass temperature is varied at two level and other four parameters (current, voltage, gas flow rate and edge including angle) are varied at three levels as shown in table 3.3.

In this study four factors are varied at three levels which makes degree of freedom (DOF) eight (DOF= number of levels – 1), one factor is varied at two levels similarly its degree of freedom become 1, hence total degree of freedom become nine. The best suited orthogonal array for mixed levels L18 orthogonal array. In L18 orthogonal array one two level and seven three level can be studied. Table 3.4 shows the allocation of degree of freedom to the factors and table 3.5 shows design of experiment.

Table 3.3: Contributing factors and there levels

S.no.	Contributing Factor	Units	Level 1	Level 2	Level 3
1	Interpass temperature	℃	100	150	
2	Welding current	Ampere	180	200	220
3	Welding voltage	Volt	22	24	26
4	Gas flow rate	Litre/minute	12	14	16
5	Edge including angle	degree	60	75	90

In this study four factors are varied at three levels which makes degree of freedom (DOF) eight (DOF= number of levels – 1), one factor is varied at two levels similarly its degree of freedom become 1, hence total degree of freedom become nine. The best suited orthogonal array for mixed levels L18 orthogonal array. In L18 orthogonal array one two level and seven three level can be studied. Table shows the allocation of degree of freedom to the factors and table 3.5 shows the design of experiment.

Table 3.4: DOF allocated to different parameters

S.no.	Contributing factor	No. of levels	Degree of freedom
1	Interpass temperature	2	1
2	Welding current	3	2
3	Welding voltage	3	2
4	Gas flow rate	3	2
5	Edge including angle	3	2
	Total DOF		9

3.3.5 Edge Preparation

In this study plates of SS304 having dimension 100 x70 x 12 mm are taken. Including edge angle is a taken as a controlling parameter in this study; it is varied at three levels 60, 75, 70 degree. Edges of plates are prepared on surface grinding machine. Plate is held in a vice at an angle according to desired groove angle using bevel square and its edge is grounded and root gap of 2 mm is maintained. Edges are prepared on 36 plates as two plates are required for each experiment according to L-18 orthogonal array. Figure 3.4 shows preparation of edges on a surface grinding machine at Thapar University, Patiala.

Table 3.5: Orthogonal array for experimentation based on L-18

S.No	Interpass Temperature '℃'	Current 'Ampere'	Voltage 'Volt'	Gas Flow Rate 'Litre/min'	Edge Including Angle 'degree'
1	100	180	22	12	60
2	100	180	24	14	75
3	100	180	26	16	90
4	100	200	22	12	75
5	100	200	24	14	90
6	100	200	26	16	60
7	100	220	22	14	60
8	100	220	24	16	75
9	100	220	26	12	90
10	150	180	22	16	90
11	150	180	24	12	60
12	150	180	26	14	75
13	150	200	22	14	90
14	150	200	24	16	60
15	150	200	26	12	75
16	150	220	22	16	75
17	150	220	24	12	90
18	150	220	26	14	60

Figure 3.4: Edge preparation of plates on surface grinding machine.

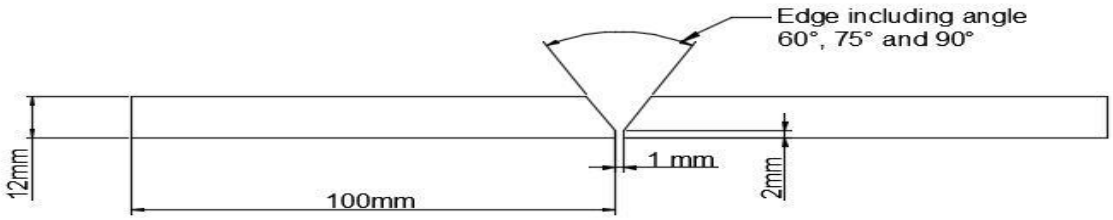

Figure 3.5: CAD design of groove geometry.

3.3.6 Joining of Plates

Plates are tacked after preparation of edges (as shown in figure 3.6) to prevent any misalignment during the welding. Groove between plates is cleaned properly with wire brush and acetone to remove any dirt and oxide layer. Welding in each experiment is done according to conditions mentioned in design of experiment. Plates are not clamped during the welding because the effect of controlling parameters on distortion of plate is taken into consideration in this study. Welding is done in three passes one root pass and subsequent two passes above it. Figure 3.5 shows CAD design of groove geometry. Interpass temperature is maintained between two pass according to design of experiment. After root pass of welding,

joint is allowed to cool to its interpass temperature and second pass of weld is made similarly when joint reached its interpass temperature third pass is made. Figure 3.7 shows plates after three passes of welding and figure 3.8 shows different passes during welding. Interpass temperature is measured using infrared thermometer gun as shown in figure 3.9. Weld joint is allowed to cool in air after welding is done. Distortion is observed in all the welds, it is measured to know the effect of controlling parameters. After measuring distortion plates are cut according to dimensions of the impact toughness, microstructure and microhardness specimen.

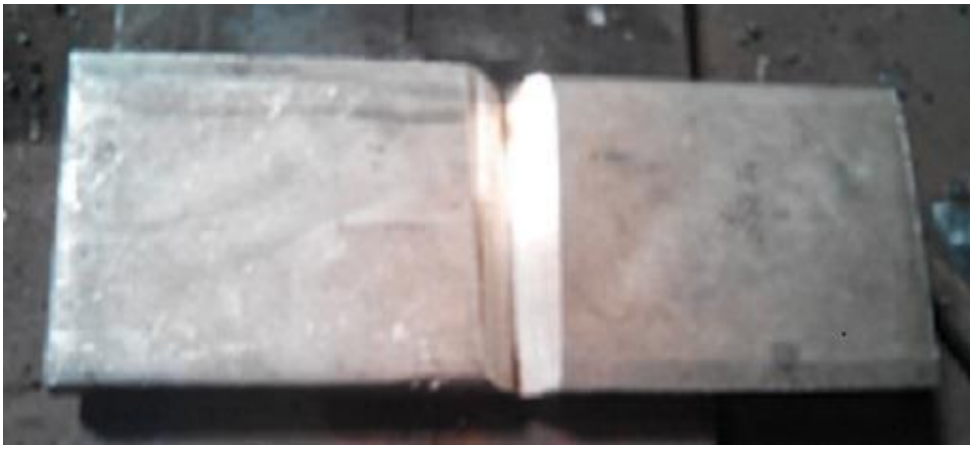

Figure 3.6: Plates after tacking

Figure 3.7: Plates after three passes of welding.

3.4 Testing of Weld Specimen

In this experimental study influence of controlling parameters are studied on austenitic stainless steel welds. Specimens for testing are prepared from weld plates after cutting. Figure 3.10 shows the scheme of cutting of samples from welded plate. Two impact test samples are prepared for testing at room temperature marked as 1, two impact test specimen

is prepared for testing at -20˚C marked as 2 and one specimen for microhardness Microstructural study is prepared marked as 3. Following tests are conducted in this study:

- Charpy Impact Test at room temperature.
- Charpy Impact Test at room temperature.
- Distortion measurement.
- Microhardness Test.
- Microstructural analysis.

	a) First pass or root pass of welding
	b) Second pass of welding
	c) Third pass of welding

Figure 3.8: Different passes during welding.

Figure 3.9: Infrared thermometer is used for maintaining interpass temperature.

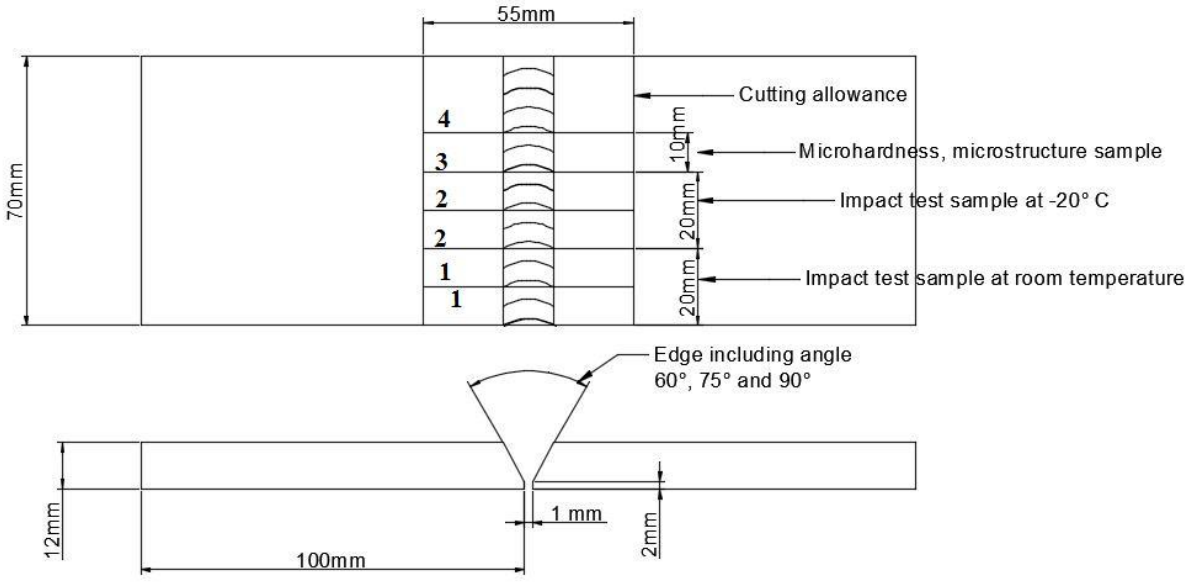

Figure 3.10: Cutting of plates after welding.

3.4.1 Impact Toughness Test

Impact toughness or impact strength is an important mechanical property for components or structures subjected to a shock loading for example in offshore industry, shipping industry, pressure vessels, aviation industry and bridges in the cold and stormy conditions. Impact toughness is a property of a weld to deform permanently and absorb energy before its fracture. Toughness of material signifies how much sudden impact energy a material can withstand before it cracks. The absorbed energy (Joule) is used as a unit for measuring the impact strength or toughness of a material.

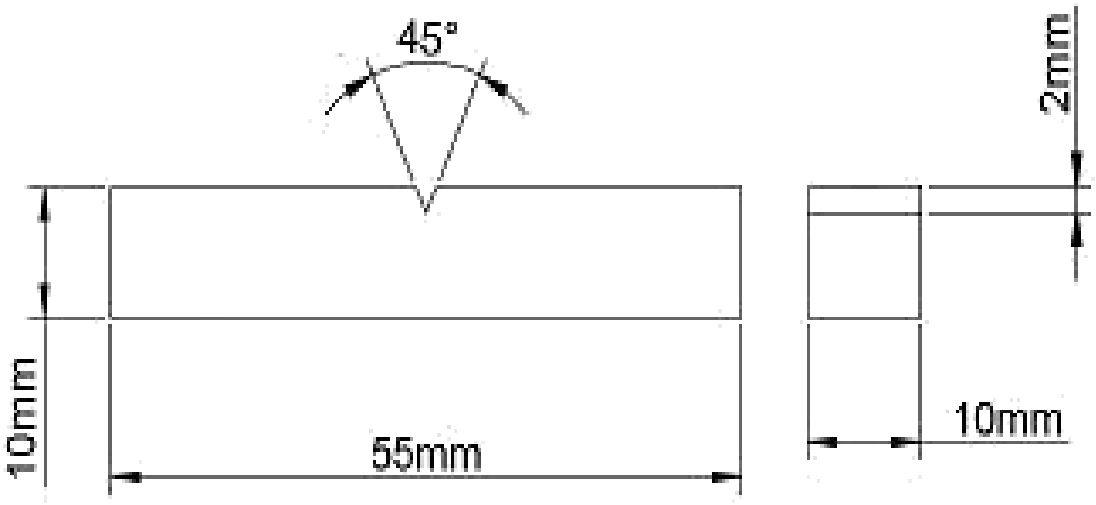

Figure 3.11 Geometric model of Charpy impact test specimen.

Sample for impact toughness is obtained from weld plates of dimension 100 x 75 x 12 mm. cutting of samples is done with leaving 1mm grinding allowance. After cutting dimensions of samples are maintained on surface grinding machine. Specimens are prepared according to ASTM A370-10 standard of size 55 x 10 x 10 mm. V notch of 45˚ angle and 2 mm depth is machined on shaper. Geometric model of impact test specimen is shown in figure 3.11. Four charpy impact test specimens are prepared from each experiment, out of which two are tested at room temperature and two are tested at -20˚ Celsius, hence total 72 impact specimens are prepared as shown in Figure 3.12. Specimens are tested on a pendulum type charpy impact testing machine; a stop pointer in machine shows how far the pendulum with hammer swings back up after striking or fracturing the specimen. Liquid nitrogen is used for testing specimens below room temperature. Samples are dipped in liquid nitrogen for 10 minutes before testing. Infrared thermometer is used to measure the temperature of samples that are tested at – 20˚ Cas shown in figure 3.13.

Figure 3.12: Charpy Impact test samples.

Figure 3.13: Infrared thermometer used to measure temperature

3.4.2 Microhardness Testing

The hardness is defined as a resistance of a material to permanent indentation. An indenter is pressed under a specific load into the surface of the material to be tested for a fixed time interval, and a size of the indentation is measured. Microhardness test is easy, simple, and non-destructive which makes it preferable. In microhardness testing value of applied loads is below 1 kg. Microhardness testing is generally done for very thin materials, very small parts, plated surfaces, superficially hardened parts, individual constituents of materials for example in composite.

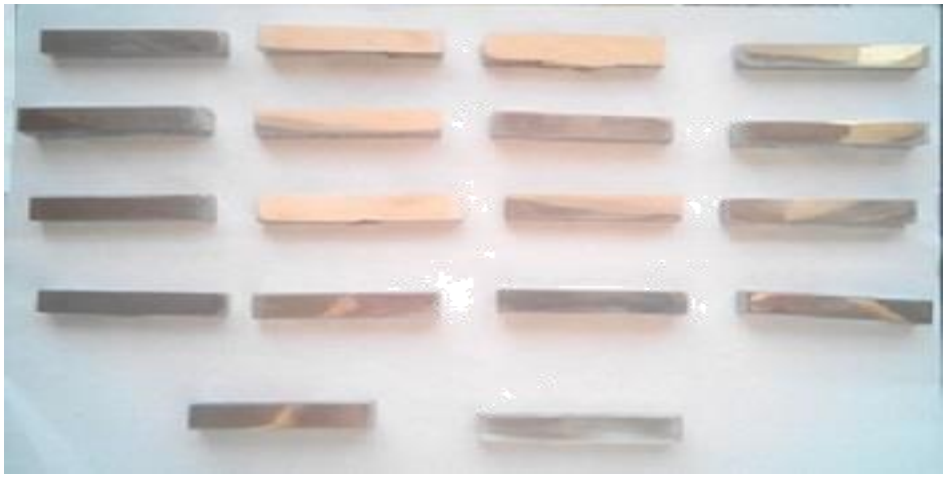

Figure 3.14: Polished specimens for microhardness and microstructural studies

a b

Figure 3.15: a) Polishing machine b) Microhardness tester

(**Courtesy:** Central Workshop, Thapar University, Patiala)

Samples for measuring microhardness is initially ground on belt grinder and polished on emery paper of coarse to fine grit size 400, 600, 800, 1000 and 2000 on a polishing machine (as shown in figure 3.15 (a)). Figure 3.14 shows polished specimens for microhardness and microstructural studies. Microhardness measurement is done on computerised vickers microhardness testing machine (Make: Metatech industries, India) as shown in figure 3.15

(b). Shape of indenter is square pyramidal in vickers microhardness test and microhardness is determined by measuring the size of this indentation. Size of indentation is measured by marking diagonal of indents using Quantimet software at magnification of 40 X, software

directly gives hardness value in hardness vickers number (HVN). Microhardness testing is done with a load of 300 grams on indenter for a dwell time of 20 seconds.

3.4.3 Distortion Measurement

Distortion occurs during welding as effect of the non-uniform cycles of expansion and contraction of the base metal and weld metal during the cooling and heating. Stresses occur in the weld due to the changes in volume of weld metal if it is not clamped properly, these stresses are able to distort the base metal and may even cause tears or fractures. Non-uniform contraction along the thickness results in angular distortion. Distortion is influenced by properties of parent metal like specific heat, thermal conductivity and coefficient of thermal expansion. Coefficient of expansion of stainless steel is higher than plain carbon steel, which makes it more prone to distortion.

Distortion is measured by the setup. After welding plate 1 and plate 2 both get distorted as shown in figure 3.16. Plate 1 is made straight using distortion measurement setup as shown in figure 3.17 and 3.18. Two points are marked on plate 2 at a fixed horizontal distance 'B' and the vertical distance 'H' between these points is measured. Using trigonometric relation the distortion angle α is calculated. Height H is measured by using digital height gauge as shown in figure 3.19.

Figure 3.16: Distorted plates after welding

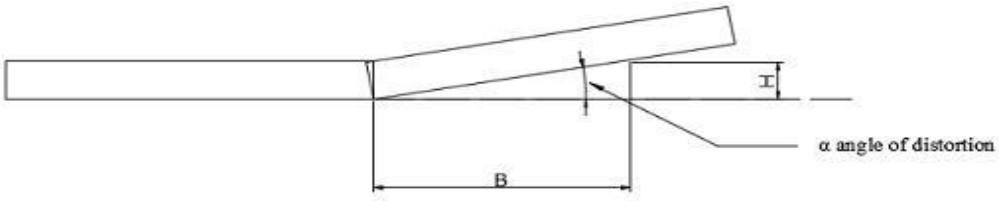

Figure 3.17: Plates held in setup for measuring distortion.

Figure 3.18: Distortion measurement setup.

Figure 3.19: Height gauge used for measuring height.

3.4.4 Microstructural Study

The microstructure of a metal influences its mechanical properties like strength, hardness toughness, ductility, wear resistance, corrosion resistance etc. these properties influences the application of materials in domestic and industrial practice. During welding source of heat interacts with material, the interaction of heat input experienced by material changes from one region to other region, which results in three different regions in the weld. These regions are the fusion zone (FZ) or the weld metal, heat-affected zone (HAZ), and base metal (BM).

Fusion zone experiences the melting and solidification of material which results in microstructural changes.

LEICA metallurgical microscope (as shown in figure 3.20) is used for microstructural images of fusion zone, fusion boundary, HAZ at a magnification of 10X, 20X and 50X. Samples are polished with the help of emery paper of coarse to fine grit size 400, 600, 800, 1000 and 2000 on a polishing machine. Samples are etched with Alder stainless steel etchant. Composition of etchant is copper ammonium chloride 9grams, hydrochloric acid 150 ml, Ferric chloride 45 grams and hydrated distilled water 75 ml. Samples are placed under lenses of different magnification for taking images. Microscope is attached with camera connected to computer, Leica software is used for image processing.

Figure 3.20: Metallurgical microscope.
(**Courtesy:** Central Workshop, Thapar University, Patiala)

The scanning electron microscopy (SEM) is used to observe the structure of fractured sample of impact toughness test. SEM (Make: JSM-6510LV, JEOL Ltd, Tokyo, Japan) is done at SAI Labs, Thapar Technology Campus, Patiala as shown in figure 3.21. In SEM the high energy beam of electron is focused on the surface of sample, various signals are generated on the surface samples. These signals are used to reveal information about the morphology, structure and composition of sample. SEM is high performance, non-destructive type of testing. Magnification of SEM is ranges between 5 to 30,000X. Chemical composition of point object can be determined by using energy dispersive spectroscopy (EDS). EDS is connected with SEM machine.

Figure 3.21: Scanning electron microscope (Courtesy; SAI Lab, Thapar University, Patiala)

3.5 Analysis of Results

Analysis of the results is done with help of analysis of variance (ANOVA) technique.

3.5.1 Analysis of Variance

ANOVA is a technique which is used to find some important conclusions from the analysis of experimental data. This technique reveals the significance level of controlling factor(s) or interaction between factors on a response. ANOVA separates the total variation of the response into the contributions of the every factor in variation and the error. So

$SS_T = SS_F + SS_E$

Where, SS_T = Total sum of squared deviations about the mean.

SS_E = Sum of squared deviations due to error.

SS_F = Sum of squared deviations due to each factor.

Mean square deviation in ANOVA table is calculated as:

$$MS = \frac{\text{Sum of squared deviations}}{\text{DOF(Degree of freedom)}}$$

F value of F ratio or Variation ratio is calculated as:

$$F = \frac{\text{MS of the factor term}}{\text{MS of the error term}}$$

On the basis of F value, P (probability of significance) value is calculated. P value decides the level of significance. Minitab 16 statistical software is used for analyzing the significance of

all the responses. The response parameters studied in this study are (1) Distortion (2) Toughness at room temperature (3) Toughness at -20℃ (4) Microhardness of fusion zone and HAZ. Degrees of freedom are used In ANOVA table for calculating the mean square (MS).

The degrees of freedom show the amount of "independent" information that is available for calculation of each sum of squares (SS). DOF of a factor is L−1 where L is number of levels of factor. In this experimental study, following response characteristics are studied

1. Response Name: Distortion
   Response type: Lower-the-better
   Units: Angle (degree)
2. Response Name: Toughness at room temperature
   Response type: Higher-the-better
   Units: Joule
3. Response Name: Toughness at -20℃
   Response type: Higher-the-better
   Units: Joule
4. Response Name: Microhardness at weld region
   Response type: Nominal-the-better
   Units: HVN

Chapter 4

Results and Discussions

4.1 Introduction

This chapter discusses the results of testing of welded specimen i.e. charpy impact test at room temperature and at -20˚C, Distortion measurement, microhardness and metallurgical study. The objective of this work is to study the influence of MIG welding input parameters i.e. interpass temperature, current, voltage, gas flow rate and edge including angle on austenitic stainless steel welds. In this chapter result of impact testing, distortion measurement and microstructural changes during the multipass MIG welding of austenitic stainless steel is studied. MINITAB 16 software is used for analysis of results using ANOVA and plotting of graphs between responses and input parameters.

4.2 Distortion

Distortion is a common phenomenon in weld joints. Distortion is result of internal stresses and residual stresses produced due to expansion and contraction of volume during heating and cooling of weld joint. Distortion of all the 18 experiments is measured using distortion measurement setup as discussed in chapter 3. Distortion in plates is measured in degree. Reading of distortion is recorded two times. Responses for each experiment, mean and signal to noise (S/N) ratio is shown in table 4.1 where

I.T. refers to interrpass temperature in℃

C refers to current in Ampere (A).

V refers to voltage in Volts (V).

G.F.R. refers to gas flow rate measured in L/min.

E.I.A refers to edge including angle measured in degree.

Table 4.1: Response table for distortion

S.No.	I.T.	C	V	G.F.R	E.I.A.	Distortion 1	Distortion 2	MEAN	S/N Ratio
1	100	180	22	12	60	6.52	6.48	6.5	-16.2583
2	100	180	24	14	75	7.53	7.418	7.474	-17.4713
3	100	180	26	16	90	8.17	8.519	8.3445	-18.4299
4	100	200	22	12	75	7.36	7.43	7.395	-17.3789
5	100	200	24	14	90	6.91	6.65	6.78	-16.6262
6	100	200	26	16	60	7.17	7.53	7.35	-17.3284
7	100	220	22	14	60	5.09	5.24	5.165	-14.2623
8	100	220	24	16	75	5.57	5.35	5.46	-14.7456
9	100	220	26	12	90	6.74	6.63	6.685	-16.5023
10	150	180	22	16	90	7.86	7.85	7.855	-17.9029
11	150	180	24	12	60	5.52	5.24	5.38	-14.6186
12	150	180	26	14	75	7.24	7.42	7.33	-17.3027
13	150	200	22	14	90	7.68	7.91	7.795	-17.8373
14	150	200	24	16	60	7.12	6.94	7.03	-16.9398
15	150	200	26	12	75	7.46	7.69	7.575	-17.5887
16	150	220	22	16	75	5.94	6.59	6.265	-15.9501
17	150	220	24	12	90	5.53	5.41	5.47	-14.7603
18	150	220	26	14	60	6.33	6.51	6.42	-16.1516

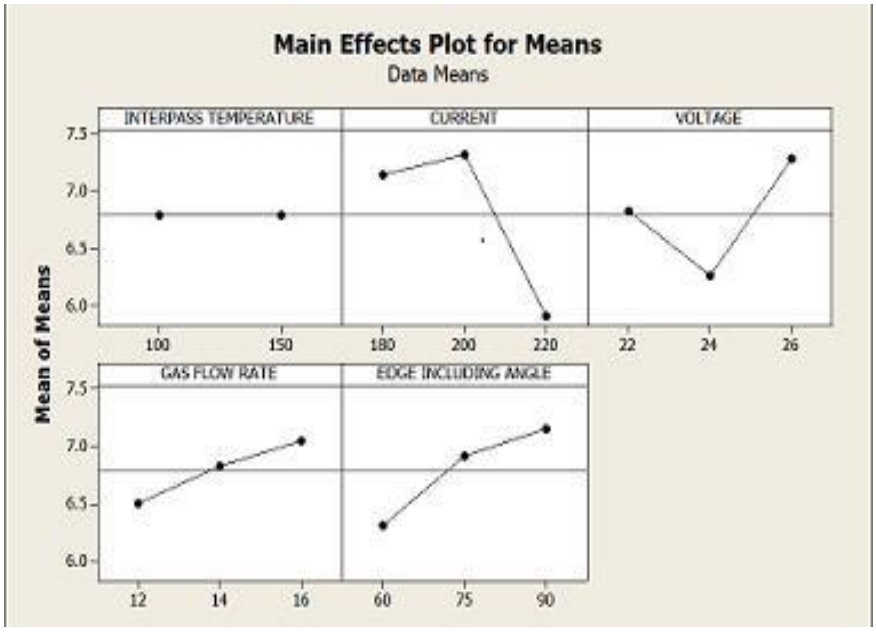

Figure 4.1: Main effect plot for means of distortion.

Figure 4.1 shows main effect plot for means of distortion. These graphs are plotted between controlling parameters and distortion values. Centerline in every graph mean of means of distortion value. Figure 4.1 shows interpass temperature has not much effect on distortion. Distortion first increases with increase in current and then decreases with increasing current. Distortion decreases with increase in voltage first and then increases with increasing voltage. Increase in distortion is shown with increase in gas flow rate. Graph between edge including angle and distortion shows increase in distortion with increase edge including angle. Increase in edge including angle means increase in amount of molten filler metal to fill groove and increase in contraction of metal during solidification which results in increase in distortion.

Table 4.2: ANOVA table for means of distortion

Source	DF	Sum of square	Variance	F Calculated	F Table	
Interpass temperature	1	0.0001	0.00006	0.00	5.32	N.S.
Current	2	7.0939	3.54696	14.98	4.46	S
Voltage	2	3.1233	1.56165	6.59	4.46	S
Gas flow rate	2	0.9179	0.45893	1.94	4.46	N.S.
Edge including angle	2	2.2917	1.14584	4.84	4.46	S
Residual Error	8	1.8944	0.23680			
Total	17	15.3212				

Table 4.3: Response table for means of distortion.

Level	Interpass temperature (A)	Current (B)	Voltage (C)	Gas flow rate (D)	Edge Including Angle (E)
1	6.795	7.147	6.829	6.501	6.308
2	6.791	7.321	6.266	6.827	6.917
3		5.911	7.284	7.051	7.155
Delta	0.004	1.410	1.018	0.550	0.847
Rank	5	1	2	4	3

Distortion response of eighteen experiments is analyzed using ANOVA. Table 4.2 shows the ANOVA table for means of distortion values. Table shows value of F calculated and F table. A parameter is considered as significant when F calculated value is larger than F table value for that parameter. F table values are at 95% confidence level. From table 4.2 three factors i.e. current, voltage and Edge including angle are significant. Table 4.3 shows average value of the five parameters. Delta values are shown in table, higher the value of this delta then

higher is the rank of that parameter. Rank 1 is most significant factor and rank 5 is least significant factor. Significance order of parameters is current, voltage, edge including angle, gas flow rate and interpass temperature higher to lower.

4.2.1 Optimal Design for Distortion

Distortion is preferred to be lower the best. Current, voltage and edge including angle are the significant parameters. B3C2E1 from Table 4.3 is the optimal condition for distortion. Optimal value for distortion is calculated as:

$\eta_{opt} = \bar{m} + (m_{B3} - \bar{m}) + (m_{C2} - \bar{m}) + (m_{E1} - \bar{m})$

$= 6.79 + (5.911 - 6.79) + (6.266 - 6.79) + (6.308 - 6.79)$

$= 6.79 - 0.879 - 0.524 - 0.482$

$= 4.905^{\circ}$

Confidence Interval (C.I.) for optimum value is

$$C.I. = \sqrt{\frac{f\,\alpha{:}v1{:}v2\ X\ Ve}{neff}}$$

α = risk (0.05) confidence = 1-α

v1 = DOF for mean (which is always 1)

v2 = DOF for error = 11

Where $f\,\alpha{:}\ v1{:}v2 = f\,0.05{:}1{:}11$ = F ratio = 4.84

$$\text{Variance (Ve)} = \frac{\text{Sum of square of error pooled}}{\text{Degree of freedom error pooled}}$$

$$(Ve) = \frac{2.8124}{11}$$

$$= 0.2557$$

n_{eff} = number of tests performed using participating factors

$$n_{eff} = \frac{18}{1+\text{DOF of } significant\ factors}$$

$$= \frac{18}{7}$$

$$= 2.57$$

C.I. = 0.694

So, confidence interval around distortion is 4.905 ± 0.694 degree.

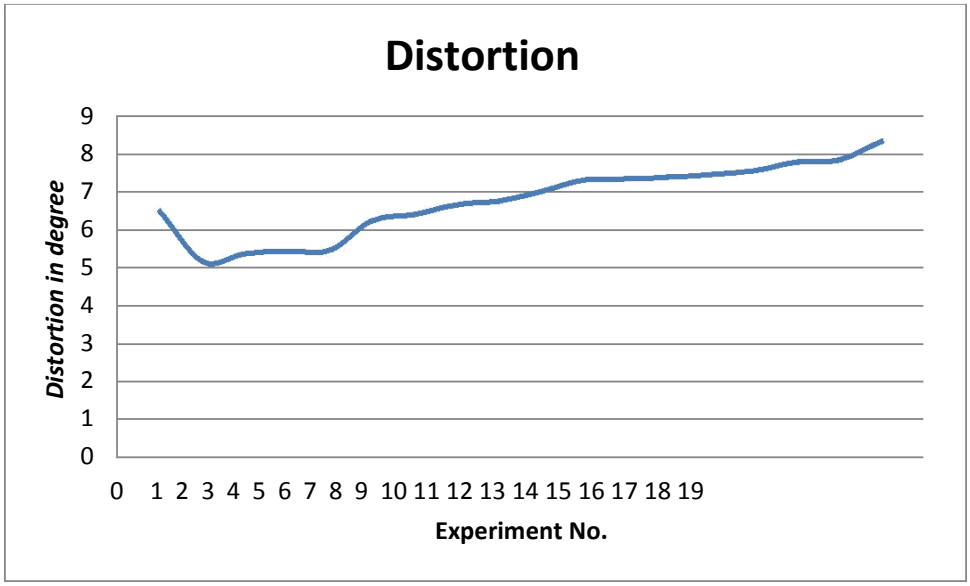

Figure 4.2: variation in distortion in experiments

4.2.2 Analysis of S/N ratio For Distortion

Higher distortion is an undesirable property in welds, so S/N ratio is calculated for lower the better option. S/N ratio for each experiment is given in Table 4.1. Table 4.4 shows the ANOVA table for S/N ratio, table shows that current and voltage are the significant factor. Table 4.5 shows the response value and rank of each factor according to its significance. According to Table 4.5 significance sequence of parameters is current, voltage, edge including angle, gas flow rate and interpass temperature higher to lower. Figure 4.3 shows the effect the effect of each controlling parameter on S/N ratio of distortion.

Table 4.4: ANOVA table for S/N ratio of distortion

Source	DF	Sum of square	Variance	F Calculated	F Table	
Interpass temperature	1	0.0001	0.00013	0.00	5.32	N.S.
Current	2	12.4236	6.21181	13.32	4.46	S
Voltage	2	5.5382	2.76908	5.94	4.46	S
Gas flow rate	2	1.4853	0.74263	1.59	4.46	N.S.
Edge including angle	2	3.8154	1.90769	4.09	4.46	N.S.
Residual Error	8	3.7312	0.46640			
Total	17	26.9938				

Table 4.5: Response Table for Signal to Noise Ratios smaller is better

Level	Interpass temperature (A)	Current (B)	Voltage (C)	Gas flow rate (D)	Edge Including Angle (E)
1	-16.56	-17.00	-16.60	-16.18	-15.93
2	-16.56	-17.28	-15.86	-16.61	-16.74
3		-15.40	-17.22	-16.88	-17.01
Delta	0.01	1.89	1.36	0.70	1.08
Rank	5	1	2	4	3

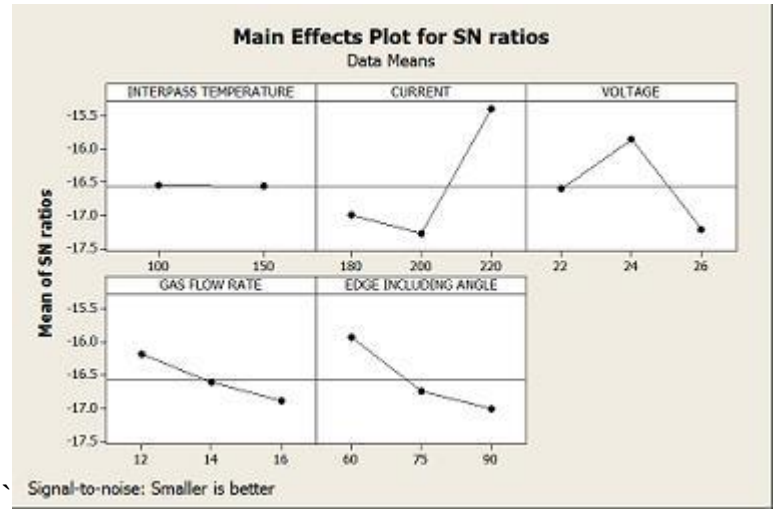

Figure 4.3: Main effect plot for S/N ratio of distortion.

4.2.3 Discussion

The effect of controlling parameters i.e. current, voltage, edge including angle, gas flow rate and interpass temperature on distortion of weld joint is studied. The smallest value of distortion is 5.165˚and largest value is 8.344˚, average of all the values is 6.793. Current, voltage and edge including angle are found as significant factor in this study. Current and voltage controls the heat input to the weld joint. Distortion is increased with increase in edge including angle. Increase in edge including angle means increase in amount of molten filler metal to fill groove and increase in contraction of metal during solidification which results in increase in distortion. Optimum value of distortion is 4.905 ± 0.694 degree at 220 A current, 24 V of voltage and 60˚edge including angle.

4.3 Impact Toughness at Room Temperature

Figure 4.4: Specimens after impact test.

Table 4.6: Response table for impact toughness at room temperature (refer Table 4.1 for experimental conditions)

Experiment no.	Impact energy (J)		Mean	S/N ratio
	Reading 1	Reading 2		
1	134	136	135	42.6060
2	168	174	171	44.6559
3	162	166	164	44.2949
4	154	132	143	43.0296
5	170	162	166	44.3946
6	168	184	176	44.8833
7	172	134	153	43.4924
8	184	174	179	45.0469
9	168	196	182	45.1243
10	134	142	138	42.7866
11	142	172	157	43.7989
12	176	150	163	44.1608
13	128	162	145	43.0479
14	174	154	164	44.2484
15	152	186	169	44.4257
16	160	194	177	44.8391
17	174	136	155	43.6104
18	188	162	175	44.7888

Impact toughness is amount of energy that a material can absorb before fracture. Figure 4.4 shows specimen after charpy impact test. Table 4.6 shows the impact energy of the specimens welded at different conditions. Two samples are prepared for each condition. Mean and signal to noise ratio is also shown in Table 4.6. Figure 4.5 shows effect of controlling parameters on the impact toughness at room temperature. Graph shows that impact toughness values vary slightly around interpass temperature. Interpass temperature has not much effect on toughness and toughness decreases with increase in interpass temperature. Impact toughness is increased with increase in current, voltage and gas flow rate. Impact energy first increases and then decrease with increase in edge including angle.

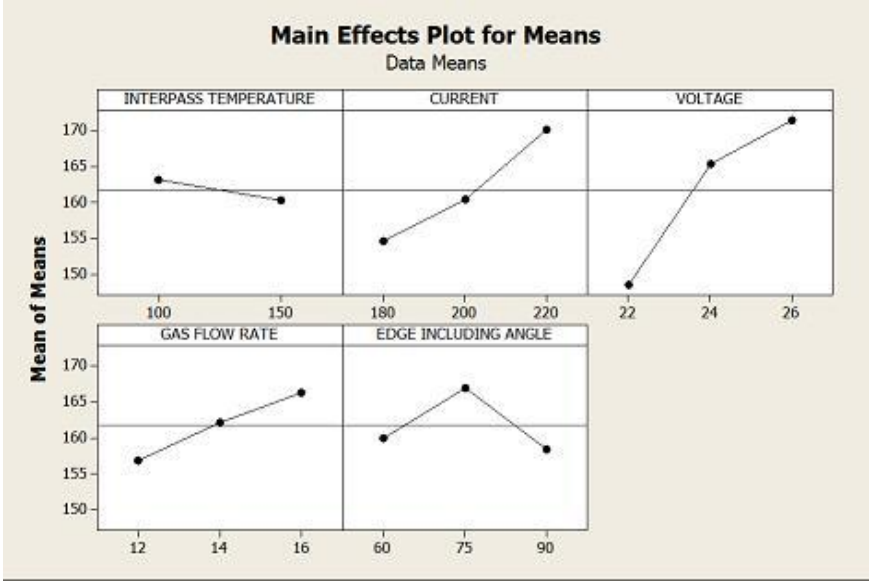

Figure 4.5: Main effect plot for means of impact toughness at room temperature.

Table 4.7: ANOVA table for means of impact toughness at room temperature

Source	DF	Sum of square	Variance	F Calculated	F Table	
Interpass temperature	1	37.56	37.56	0.55	5.32	N.S.
Current	2	735.44	367.72	5.41	4.46	S
Voltage	2	1700.78	850.39	12.52	4.46	S
Gas flow rate	2	272.11	136.06	2.00	4.46	N.S.
Edge including angle	2	253.78	126.89	1.87	4.46	N.S.
Residual Error	8	543.44	67.93			
Total	17	3543.11				

Table 4.8: Response table for means of impact toughness at room temperature

Level	Interpass temperature (A)	Current (B)	Voltage (C)	Gas flow rate (D)	Edge Including Angle (E)
1	163.2	154.7	148.5	156.8	160.0
2	160.3	160.5	165.3	162.2	167.0
3		170.2	171.5	166.3	158.3
Delta	2.9	15.5	23.0	9.5	8.7
Rank	5	2	1	3	4

Table 4.7 shows ANOVA table for means of impact toughness at room temperature.voltage and current has F calculated value larger than F table value at 95 % significance level; hence voltage and current are significant factor. Table 4.8 shows response table for means of impact toughness at room temperature. Delta values are shown in table, higher the value of this delta then higher is the rank of that parameter. Rank 1 is most significant factor and rank 5 is least significant factor. Significance sequence of parameters is voltage, current, gas flow rate, edge including angle and interpass temperature higher to lower.

4.3.1 Optimal Design for Impact Toughness at Room Temperature

Toughness is preferred to be higher the better. Voltage and current are the significant parameters from Table 4.7. B3C3 from Table 4.8 is the optimal condition for impact toughness at room temperature. Optimal value for impact toughness at room temperature is calculated as:

$$\eta_{opt} = \bar{m} + (m_{B3} - \bar{m}) + (m_{C3} - \bar{m})$$

$$= 161.77 + (170.2 - 161.77) + (171.5 - 161.77)$$

$$= 161.77 + 8.43 + 9.73$$

$$= 179.93 \text{ J}$$

Confidence Interval (C.I.) for optimum value is

$$\text{C.I.} = \sqrt{\frac{f\,\alpha{:}v1{:}v2\ X\ Ve}{neff}}$$

α = risk (0.05) confidence = 1-α

v1 = DOF for mean (which is always 1)

v2 = DOF for error = 13

Where $f\,\alpha{:}\ v1{:}v2 = f\,0.05{:}1{:}13$ = F ratio = 4.67

$$\text{Variance (Ve)} = \frac{\text{Sum of square of error pooled}}{\text{Degree of freedom error pooled}}$$

$$(Ve) = \frac{1106.89}{13}$$

$$= 85.145$$

n_{eff} = number of tests performed using participating factors

$$n_{eff} = \frac{18}{1+\text{DOF of } significant\ factors}$$

$$= \frac{18}{5}$$

$$= 3.6$$

C.I. = 10.51

So, confidence interval around distortion is 179.93 ± 10.51 J.

4.3.2 Analysis of S/N ratio For Impact Toughness at Room Temperature

Impact toughness is desired to be higher in weld joint, so S/N ratio is calculated for higher the better option. S/N ratio for each experiment is given in Table 4.6. Table 4.10 shows the ANOVA table for S/N ratio, table shows that current and voltage are the significant factor. Table 4.9 shows the response value and rank of each factor according to its significance. According to Table 4.9 significance sequence of parameters is voltage, current, gas flow rate edge including angle, and interpass temperature higher to lower. Figure 4.6 shows the effect of each controlling parameter on S/N ratio of impact toughness test.

Table 4.9: Response Table for Signal to Noise Ratio larger is better

Level	Interpass temperature (A)	Current (B)	Voltage (C)	Gas flow rate (D)	Edge Including Angle (E)
1	44.17	43.72	43.30	43.77	43.97
2	43.97	44.00	44.29	44.09	44.36
3		44.48	44.61	44.35	43.88
Delta	0.20	0.77	1.31	0.58	0.48
Rank	5	2	1	3	4

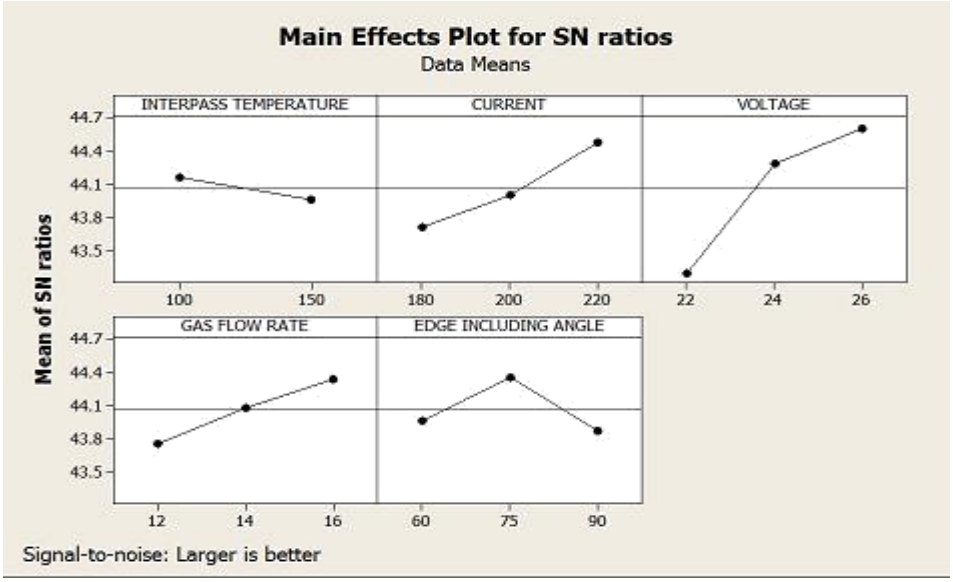

Figure 4.6: Main effect plot for S/N ratio of impact toughness at room temperature.

Table 4.10: ANOVA table for S/N ratio of Impact toughness at room temperature

Source	DF	Sum of square	Variance	F Calculated	F Table	
Interpass temperature	1	0.1843	0.1843	0.91	5.32	N.S.
Current	2	1.7988	0.8994	4.45	4.46	S
Voltage	2	5.6210	2.8105	13.90	4.46	S
Gas flow rate	2	1.0277	0.5138	2.54	4.46	N.S.
Edge including angle	2	0.7886	0.3943	1.95	4.46	N.S.
Residual Error	8	1.6170	0.2021			
Total	17	11.0374				

4.3.3 Discussion

The effect of controlling parameters i.e. current, voltage, edge including angle, gas flow rate and interpass temperature on impact toughness of weld joint is studied. The smallest value of impact toughness is 135 J and largest value is 182 J, mean of all the values is 161.778 J. Figure 4.7 shows variation in toughness values in trials. Voltage and Current are found as significant factor in this study. Voltage and current controls the heat input to the weld joint. Toughness is increased with increase in voltage and current. Increase in current increases the

penetration which improves toughness and increase in voltage results in increase in fusion zone. Optimum value of toughness is 179.93 ± 10.51 J at 220 A current and 26 V of voltage.

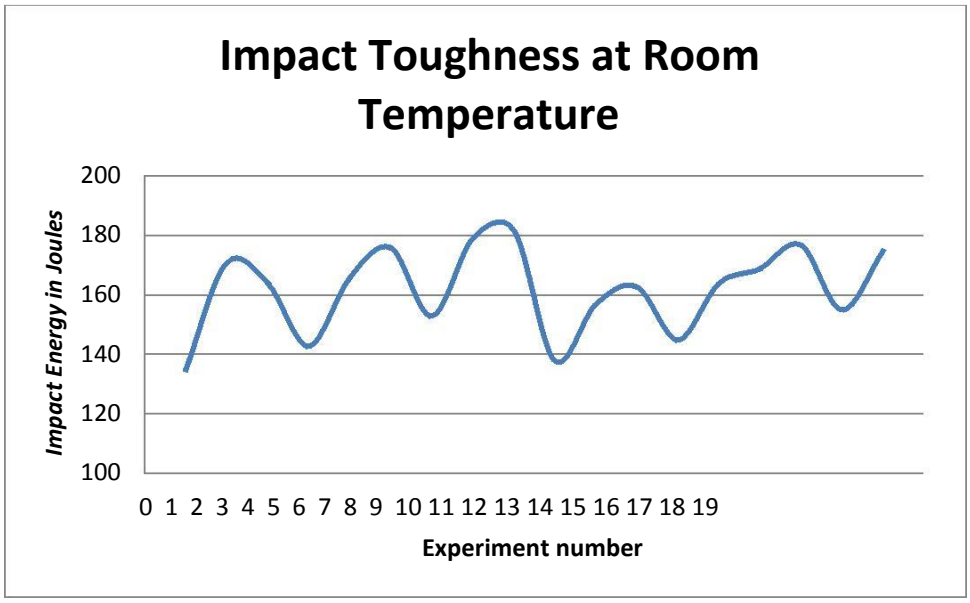

Figure 4.7: Variation in impact toughness at room temperature.

4.4 Impact Toughness at – 20℃ Temperature

Table 4.11: Response table for impact toughness at -20˚C
(refer Table 4.1 for experimental conditions)

Experiment no.	Impact Toughness (J)		Mean	S/N Ratio
	Reading 1	Reading 2		
1	108	112	110	40.8235
2	144	152	148	43.3957
3	142	148	145	43.2218
4	126	108	117	41.2865
5	144	156	150	43.5010
6	146	168	157	43.8540
7	144	108	126	41.7406
8	160	148	154	43.7306
9	146	176	161	44.0233
10	106	116	111	40.8800
11	120	148	134	42.3996
12	156	128	142	42.9189
13	104	136	120	41.3513
14	150	128	139	42.7786
15	130	164	147	43.1717
16	148	136	142	43.0225
17	174	136	155	43.6104
18	188	162	175	44.7888

Impact toughness of a material is decreased with decrease in temperature. Table 4.11 shows the impact energy of the specimens welded at different conditions. Two samples are prepared for each condition. Mean and signal to noise ratio is also shown in Table 4.11. Figure 4.8 shows effect of controlling parameters on the impact toughness at below room temperature. Toughness decreases with increase in interpass temperature. Impact toughness is increased with increase in current, voltage and gas flow rate. Impact energy first increases and then decrease with increase in edge including angle. Interpass temperature, gas flow rate and edge including angle vary close to mean line, this signifies these factors are not much significant.

Table 4.12: ANOVA table for means of Impact toughness at -20˚C

Source	DF	Sum of square	Variance	F Calculated	F Table	
Interpass temperature	1	60.50	0.2799	1.64	5.32	N.S.
Current	2	725.44	1.3638	9.85	4.46	S
Voltage	2	3036.11	6.6216	41.21	4.46	S
Gas flow rate	2	98.78	0.2927	1.34	4.46	N.S.
Edge including angle	2	75.44	0.2211	1.02	4.46	N.S.
Residual error	8	294.67	0.1759			
Total	17	4290.94				

Table 4.13: Response Table for means larger is better

Level	Interpass temperature (A)	Current (B)	Voltage (C)	Gas flow rate (D)	Edge Including Angle (E)
1	140.9	131.7	121.0	135.8	136.7
2	137.2	138.3	145.2	140.0	141.7
3		147.2	151.0	141.3	138.8
Delta	3.7	15.5	30	5.5	5.0
Rank	5	2	1	3	4

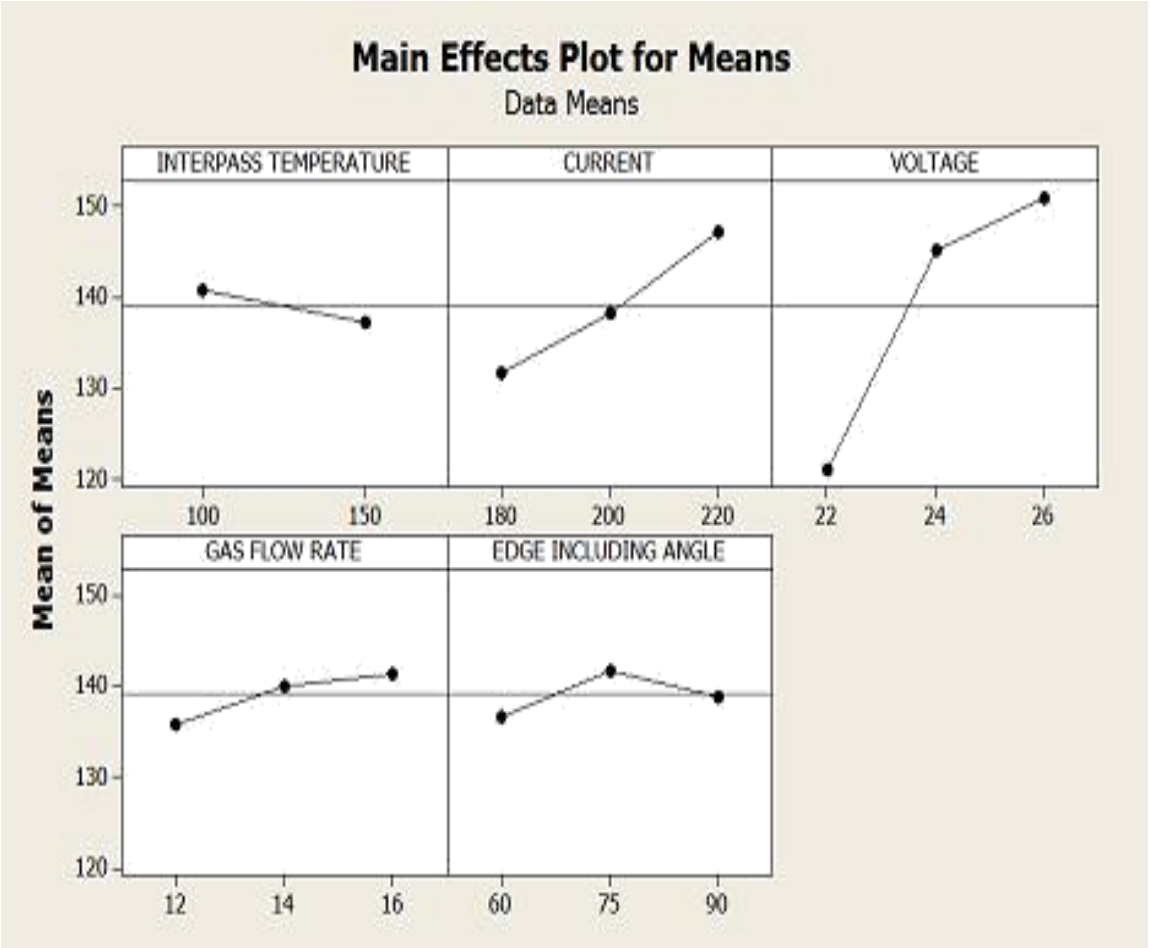

Figure 4.8: Main effect plot for means of impact toughness at – 20℃

Table 4.12 shows ANOVA table for means of impact toughness at room temperature. Voltage and current has F calculated value larger than F table value at 95 % significance level; hence voltage and current are significant factor. Table 4.13 shows response table for means of impact toughness at – 20˚C. Delta values are shown in table, higher the value of this delta then higher is the rank of that parameter. Rank 1 is most significant factor and rank 5 is least significant factor. Significance sequence of parameters is voltage, current, gas flow rate, edge including angle and interpass temperature higher to lower.

4.4.1 Optimal Design for Impact Toughness at – 20℃.

Toughness is preferred to be higher the best. Voltage and current are the significant parameters from Table 4.7. B3C3 from Table 4.8 is the optimal condition for impact toughness at room temperature. Optimal value for impact toughness at room temperature is calculated as:

$$\eta_{opt} = \bar{m} + (m_{B3} - \bar{m}) + (m_{C3} - \bar{m})$$

= 140.72 + (147.2 – 161.77) + (151.5 – 161.77)

= 161.77 – 14.57 – 10.27

= 136.93 J

Confidence Interval (C.I.) for optimum value is

$$C.I. = \sqrt{\frac{f\,\alpha{:}v1{:}v2\ X\ Ve}{neff}}$$

α = risk (0.05) confidence = 1-α

v1 = DOF for mean (which is always 1)

v2 = DOF for error = 13

Where $f\,\alpha{:}\ v1{:}v2 = f\,0.05{:}1{:}13$ = F ratio = 4.67

$$\text{Variance (Ve)} = \frac{\text{Sum of square of error pooled}}{\text{Degree of freedom error pooled}}$$

$$(Ve) = \frac{529.39}{13}$$

= 40.72

n_{eff} = number of tests performed using participating factors

$$n_{eff} = \frac{18}{1+\text{DOF of } significant\ factors}$$

$$= \frac{18}{5}$$

$$= 3.6$$

C.I. = 7.27

So, confidence interval around distortion is 136.93 ± 7.27 J.

4.4.2 Analysis of S/N ratio For Impact toughness at – 20℃

Impact toughness is desired to be higher in weld joint, so S/N ratio is calculated for higher the better option. S/N ratio for each experiment is given in Table 4.11. Table 4.14 shows the ANOVA table for S/N ratio, table shows that current and voltage are the significant factor. Table 4.15 shows the response value and rank of each factor according to its significance. According to Table 4.15 significance sequence of parameters is voltage, current, gas flow rate edge including angle, and interpass temperature higher to lower. Figure 4.9 shows the effect of each controlling parameter on S/N ratio of impact toughness test.

Table 4.14: ANOVA table for S/N ratio of Impact toughness at -20˚C

Source	DF	Sum of square	Variance	F Calculated	F Table	
Interpass temperature	1	0.2799	0.2799	1.59	5.32	N.S.
Current	2	2.7276	1.3638	7.75	4.46	S
Voltage	2	13.2433	6.6216	37.64	4.46	S
Gas flow rate	2	0.5854	0.2927	1.66	4.46	N.S.
Edge including angle	2	0.4422	0.2211	1.26	4.46	N.S.
Residual error	8	1.4072	0.1759			
Total	17	18.6857				

Table 4.15: Response Table for Signal to Noise Ratios larger is better.

Level	Interpass temperature (A)	Current (B)	Voltage (C)	Gas flow rate (D)	Edge Including Angle (E)
1	42.84	42.27	41.52	42.48	42.54
2	42.59	42.66	43.16	42.76	42.92
3		43.22	43.47	42.91	42.69
Delta	0.25	0.95	1.95	0.44	0.38
Rank	5	2	1	3	4

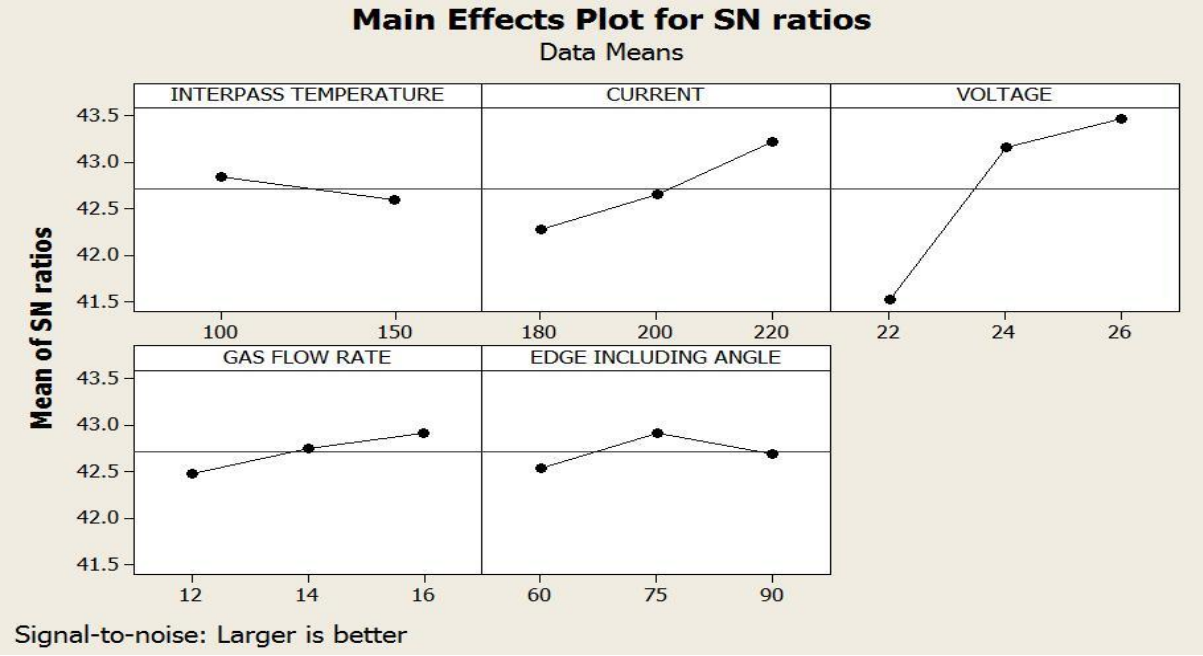

Figure 4.9: Main effect plot for S/N ratio of impact toughness at – 20℃.

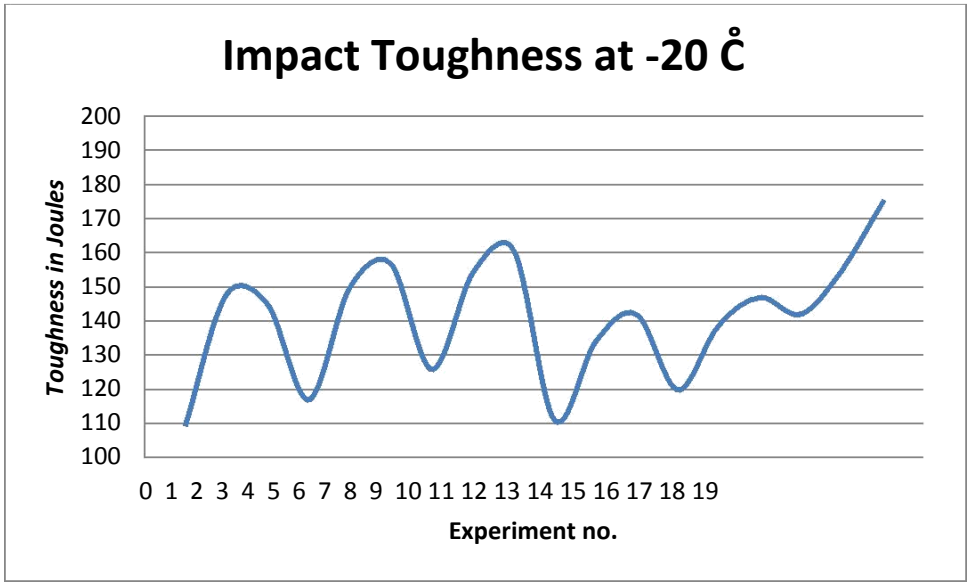

Figure 4.10: Variation in impact toughness at – 20℃

4.4.3 Discussion

The effect of controlling parameters i.e. current, voltage, edge including angle, gas flow rate and interpass temperature on impact toughness of weld joint at – 20˚C is studied. The smallest value of impact toughness is 110 J and largest value is 175 J mean of all the values is 140.722 J. Figure 4.10 shows variation in toughness values in trials. Voltage and Current are found as significant factor in this study. Voltage and current controls the heat input to the weld joint. Toughness is increased with increase in voltage and current. Increase in current increases the penetration which improves toughness and increase in voltage results in increase in fusion zone. Values of impact toughness are lower at – 20˚C than at room temperature. Impact toughness values decrease with decrease in temperature because of ductile to brittle transition. Optimums value of impact toughness at – 20˚C is 136.93 ± 7.27 J at 220 A current and 26 V of voltage.

4.5 Microhardness of Fusion Zone

Microhardness of a material is a property of a material to resist indentation. Microhardness is done by load under 1 Kg, testing was done at 300 grams in this study. Table 4.16 shows the microhardness of the specimens welded at different conditions. Figure 4.11 shows effect of controlling parameters on the microhardness of fusion zone. Microhardness increases with increase in interpass temperature and voltage. Microhardness first increases and then decrease

with increase in current. Gas flow rate and edge including angle vary close to mean line, this signifies these factors are not much significant.

Table 4.16: Response table for microhardness of fusion zone
(refer Table 4.1 for experimental conditions).

Experiment no.	Microhardness of fusion zone(VHN)			Mean
	Reading 1	Reading 2	Reading 3	
1	218.895	220.701	221.357	220.317
2	276.233	278.356	276.755	277.114
3	334.544	337.936	335.802	336.094
4	242.249	245.257	246.354	244.620
5	298.348	303.295	294.776	298.806
6	368.723	372.676	369.753	370.384
7	250.443	246.143	242.235	246.273
8	298.348	304.141	303.295	301.928
9	346.267	342.526	345.556	344.783
10	250.443	257.106	255.151	254.233
11	305.140	310.104	313.152	309.465
12	355.672	359.386	353.519	356.192
13	276.755	274.222	279.434	276.803
14	337.936	335.375	334.544	335.951
15	402.226	405.536	406.538	404.766
16	255.152	257.425	260.489	257.688
17	316.447	313.152	316.447	315.348
18	332.418	339.237	339.237	336.964

Table 4.17: ANOVA table for means of microhardness of fusion zone

Source	DF	Sum of square	Variance	$F_{Calculated}$	F_{Table}	Source
Interpass temperature	1	2382.7	2382.7	13.14	5.32	S
Current	2	2810.2	1405.1	7.75	4.46	S
Voltage	2	35148.7	17574.4	96.91	4.46	S
Gas flow rate	2	368.0	184.0	1.01	4.46	N.S.
Edge including angle	2	46.4	23.2	0.13	4.46	N.S.
Residual Error	8	1450.8	181.3			
Total	17	42206.7				

Table 4.18: Response Table for means of microhardness of fusion zone

Level	Interpass temperature (A)	Current (B)	Voltage (C)	Gas flow rate (D)	Edge Including Angle (E)
1	293.4	292.2	250.0	306.6	303.2
2	316.4	321.9	306.4	298.7	307.1
3		300.5	358.2	309.4	304.3
Delta	23.0	29.7	108.2	10.7	3.8
Rank	3	2	1	4	5

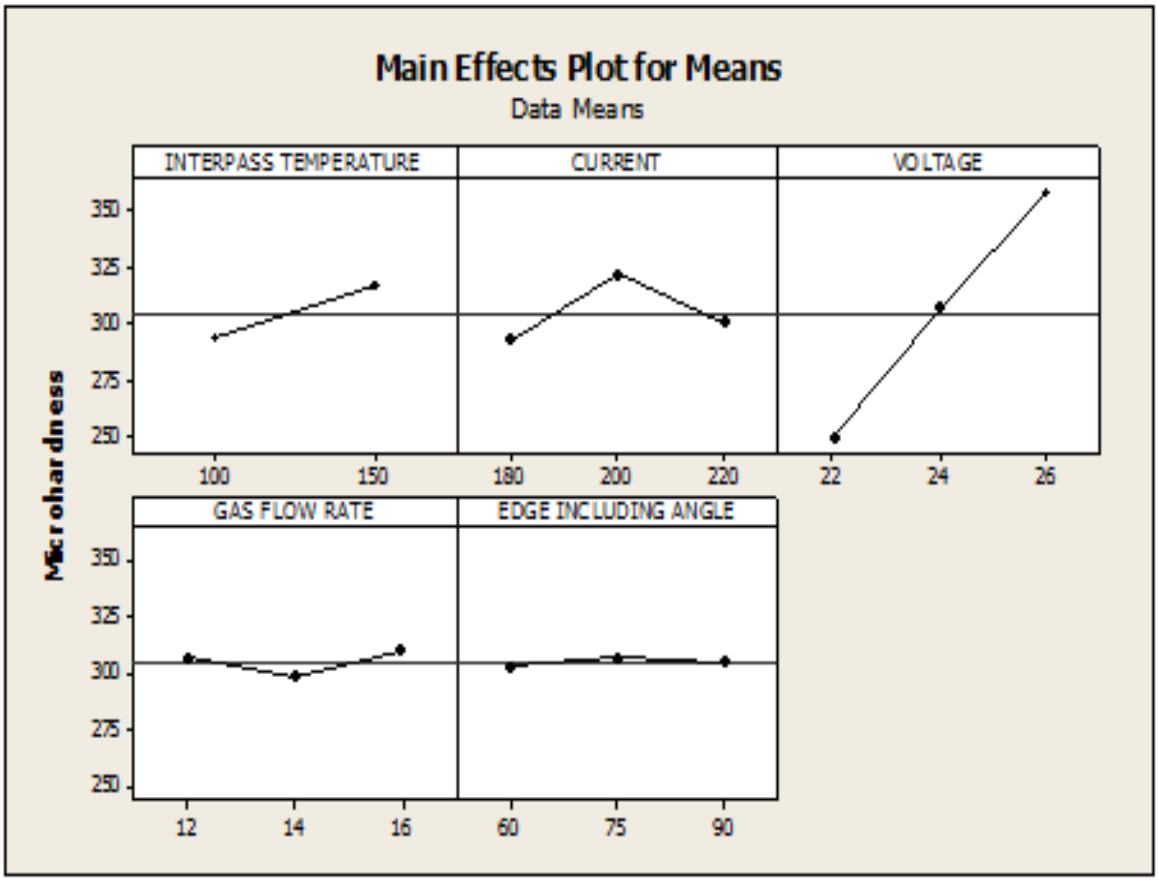

Figure 4.11: Main effect plot for means of microhardness of fusion zone.

Table 4.17 shows ANOVA table for means of microhardness at fusion zone. Voltage, interpass temperature and current have F calculated value larger than F table value at 95 % significance level; hence voltage, interpass temperature and current are significant factor. Table 4.18 shows response table for means of microhardness of fusion zone. Delta values are shown in table, higher the value of this delta then higher is the rank of that parameter. Rank 1

is most significant factor and rank 5 is least significant factor. Significance sequence of parameters is voltage, current, interpass temperature, gas flow rate and edge including angle higher to lower.

4.5.1 Optimal Design for microhardness at fusion zone

Microhardness is optimised for nominal the better. Voltage, interpass temperature and current are the significant parameters from Table 4.17. A1B2C2 from Table 4.18 is the optimal condition for microhardness of fusion zone. Optimal value for microhardness of fusion zone is calculated as:

$\eta_{opt} = \bar{m} + (m_{A1} - \bar{m}) + (m_{B2} - \bar{m}) + (m_{C2} - \bar{m})$

$= 304.87 + (293.4 - 304.87) + (321.9 - 304.87) + (306.4 - 304.87)$

$= 304.87 - 11.47 + 17.07 + 1.53$

$= 312$ HVN

Confidence Interval (C.I.) for optimum value is

$$C.I. = \sqrt{\frac{f\,\alpha:v1:v2\ X\ Ve}{neff}}$$

α = risk (0.05) confidence = 1-α

v1 = DOF for mean (which is always 1)

v2 = DOF for error = 12

Where $f\,\alpha: v1:v2 = f\,0.05:1:12$ = F ratio = 4.75

$$\text{Variance (Ve)} = \frac{\text{Sum of square of error pooled}}{\text{Degree of freedom error pooled}}$$

$$(Ve) = \frac{1865.2}{12}$$

$= 155.43$

n_{eff} = number of tests performed using participating factors

$$n_{eff} = \frac{18}{1+\text{DOF of } significant\ factors}$$

$$= \frac{18}{6}$$

$= 3$

C.I. = 54.34

So, confidence interval around microhardness of fusion zone is 312 ± 54.34 HVN.

4.5.2 Discussion

The effect of controlling parameters i.e. current, voltage, edge including angle, gas flow rate and interpass temperature on microhardness of fusion is studied. The smallest value of microhardness is 220 VHN and largest value is 404.67 VHN mean of all the values is 304.87 VHN. Voltage, interpass temperature and current are found as significant factor in this study. Voltage and current controls the heat input, cooling rate and microstructure of the weld joint change in microstructure affects microhardness. Microhardnessss is increased with increase in voltage and interpass temperature. Microhardness first increased with increase in current and then decreased. Optimum value of microhardness is 312 ± 54.34 HVN at 200 A current, 24 V of voltage and 100˚C of interpass temperature.

4.6 Microhardness of Heat Effected Zone

Microhardness of a material is a property of a material to resist indentation. Microhardness is done by load under 1 Kg, testing was done at 300 grams in this study. Table 4.19 shows the microhardness of the specimens welded at different conditions. Figure 4.12 shows effect of controlling parameters on the microhardness of fusion zone. Microhardness increases with increase in interpass temperature and voltage. Microhardness first increases and then decrease with increase in current. Microhardness of heat affected zone first decreases and then increases with increase in gas flow rate. Microhardness first increased and then decreased with increase in edge including error.

Table 4.21 shows ANOVA table for means of microhardness at heat affected zone. Voltage, interpass temperature and current have F calculated value larger than F table value at 95 % significance level; hence voltage, interpass temperature and current are significant factor. Table 4.20 shows response table for means of microhardness of fusion zone. Delta values are shown in table, higher the value of this delta then higher is the rank of that parameter. Rank 1 is most significant factor and rank 5 is least significant factor. Significance sequence of parameters is voltage, current, interpass temperature, edge including angle and gas flow rate higher to lower.

Table 4.19: Response table for microhardness of heat affected zone (refer Table 4.1 for experimental conditions).

Experiment no.	Microhardness of HAZ (VHN)			Mean
	Reading 1	Reading 2	Reading 3	
1	310.104	313.152	315.348	312.868
2	327.923	331.211	332.418	330.5173
3	387.098	384.547	387.098	386.2477
4	349.565	351.001	346.268	348.9447
5	334.548	337.9356	339.463	337.3155
6	402.226	406.733	405.536	404.8317
7	244.383	248.275	245.257	245.9717
8	322.569	316.244	320.474	319.7623
9	397.794	393.435	392.774	394.6677
10	324.684	327.853	326.236	326.2577
11	339.237	342.752	348.353	343.4473
12	399.965	408.908	403.648	404.1737
13	372.677	370.831	368.722	370.7433
14	384.928	389.147	386.348	386.8077
15	445.68	445.68	450.939	447.4330
16	364.831	362.677	365.368	364.2920
17	306.773	303.764	307.519	306.0187
18	393.435	397.563	394.647	395.2150

Table 4.20: Response Table for means of microhardness of heat affected zone

Level	Interpass temperature (A)	Current (B)	Voltage (C)	Gas flow rate (D)	Edge Including Angle (E)
1	342.3	350.6	328.2	358.9	348.2
2	371.6	382.7	337.3	347.3	369.2
3		337.7	405.4	364.7	353.5
Delta	29.3	45.0	77.2	17.4	21.0
Rank	3	2	1	5	4

Table 4.21: ANOVA table for means of microhardness of heat affected zone

Source	DF	Sum of square	Variance	F Calculated	F Table	Source
Interpass temperature	1	3850.4	3850.4	7.60	5.32	S
Current	2	6448.9	3224.5	6.37	4.46	S
Voltage	2	21381.2	10690.6	21.11	4.46	S
Gas flow rate	2	939.2	469.6	0.93	4.46	N.S.
Edge including angle	2	1428.6	714.3	1.41	4.46	N.S.
Residual Error	8	4051.4	506.4			
Total	17	38099.7				

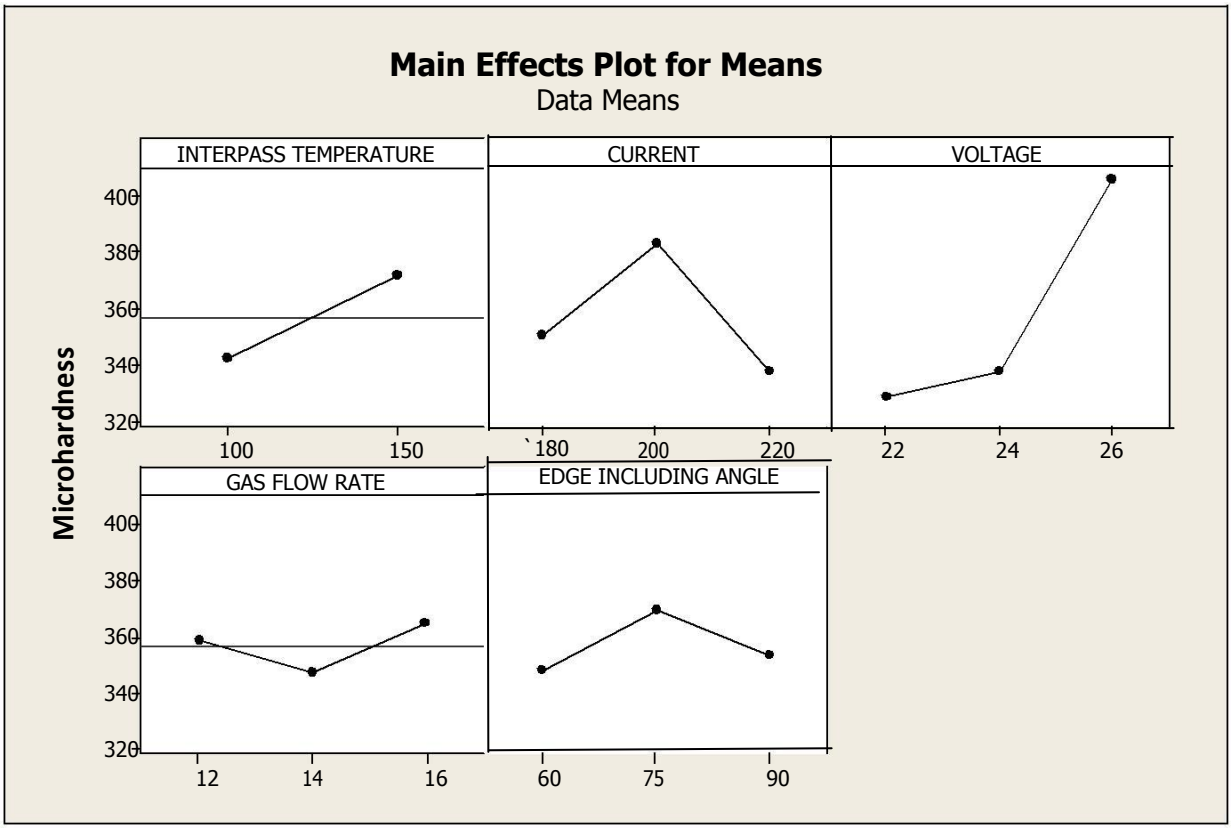

Figure 4.12: Main effect plot for means of microhardness of heat affected zone.

4.6.1 Optimal Design for microhardness at heat affected zone.

Microhardness is optimised for nominal the better. Voltage, interpass temperature and current are the significant parameters from Table 4.17. A1B1C2 from Table 4.18 is the optimal condition for impact toughness at room temperature. Optimal value for microhardness of heat affected zone is calculated as:

$\eta_{opt} = \bar{m} + (m_{A1} - \bar{m}) + (m_{B2} - \bar{m}) + (m_{C2} - \bar{m})$

$= 356.97 + (342.3 - 356.97) + (350.6 - 356.97) + (337.3 - 356.97)$

$= 356.97 - 14.67 - 6.37 - 19.67$

$= 316.26$ HVN

Confidence Interval (C.I.) for optimum value is

$$C.I. = \sqrt{\frac{f\ \alpha:v1:v2\ X\ Ve}{neff}}$$

α = risk (0.05) confidence = 1-α

v1 = DOF for mean (which is always 1)

v2 = DOF for error = 12

Where $f\ \alpha: v1:v2 = f\ 0.05:1:12$ = F ratio = 4.75

$$\text{Variance (Ve)} = \frac{\text{Sum of square of error pooled}}{\text{Degree of freedom error pooled}}$$

$$(Ve) = \frac{6419.2}{12}$$

$= 534.93$

n_{eff} = number of tests performed using participating factors

$$n_{eff} = \frac{18}{1+\text{DOF of } significant\ factors}$$

$$= \frac{18}{6}$$

$= 3$

C.I. = 29.10

So, confidence interval around distortion is 316.26 ± 29.10 HVN.

4.6.2 Discussion

The effect of controlling parameters i.e. current, voltage, edge including angle, gas flow rate and interpass temperature on microhardness of heat affected zone is studied. The smallest value of microhardness is 245.97 VHN and largest value is 447.43 VHN mean of all the values is 356.97 VHN. Voltage, interpass temperature and Current are found as significant factor in this study. Voltage and current controls the heat input, cooling rate and microstructure of the weld joint change in these properties affects microhardness. Microhardnessss is increased with increase in voltage and interpass temperature. Microhardness first increased with increase in current and then decreased. Optimum value of microhardness is 316.26 ± 29.10 HVN at 200 A current, 24 V of voltage and 100˚C of interpass temperature.

4.7 Metallurgical Study

Polished and etched samples are observed under LEICA metallurgical microscope at a magnification of 10X, 20X and 50X. Table 4.22 shows optical micrographs of samples prepared for all trial conditions at different magnifications. In table 4.22, first coulmn shows the experiment number, for experimental condition of any experiment can be referred from table 4.1, rest of the columns in table 4.22 shows micrographs at different magnification (10X, 20X and 50X) for an experimental condition. These microstructure shows different zones i.e. fusion zone, fusion boundary, heat affected zone and base metal. All the zones are clearly distinguishable because of different grain structure. Fusion zone in all the samples is majorly dendritic. Grain growth is perpendicular to the boundary of molten pool because of highest thermal gradient and maximum heat extraction at fusion boundary. Solidification mode from base metal to fusion zone changes from planar to cellular to dendritic, but most of the fusion zone has dendritic structure as shown in micrographs. Size of fusion zone and heat affected zone is increased with increase in heat input. Light colour in microstructure shows austenite phase and dark coloured structure is delta ferrite in austenitic matrix, lathy ferrite is also present in some portion of micrographs. Fusion zone is having fine structure and heat affected zone is coarser than the fusion zone. Inter dendritic spacing in some samples (6, 8 and 13) is higher than other samples.

Tables 4.22: Optical micrographs of weld joint for different experimental trials

	10X	20X	50X
1	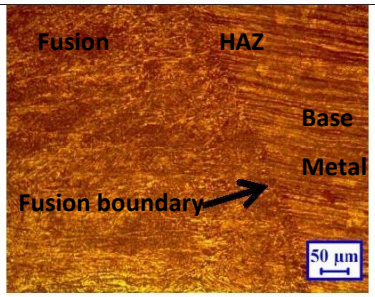	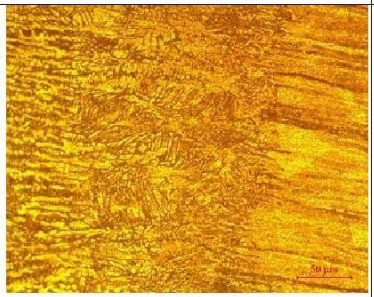	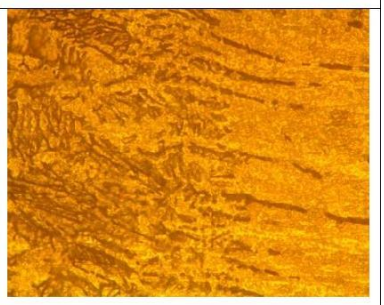
2	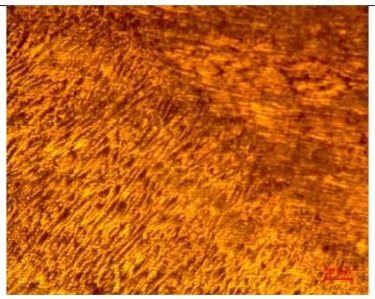	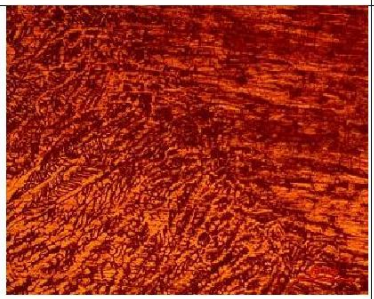	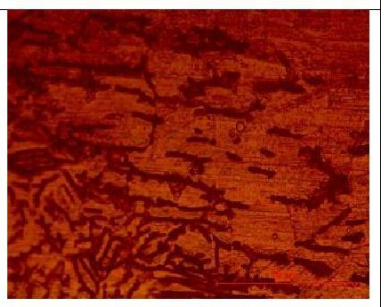
3	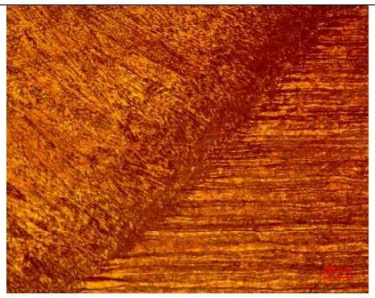	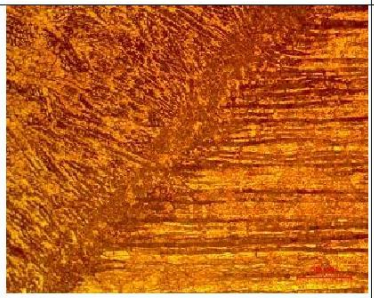	
4	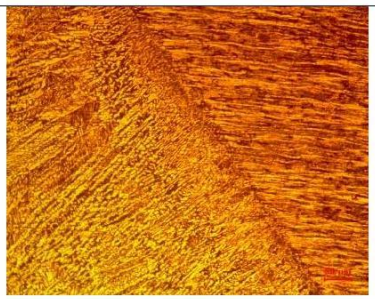	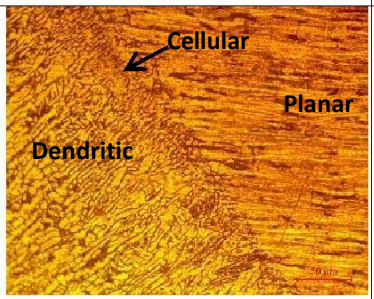	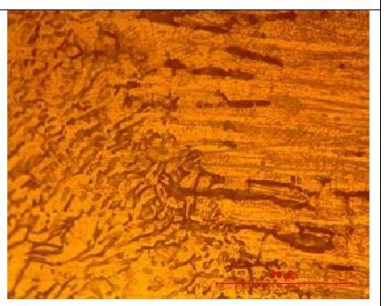
5	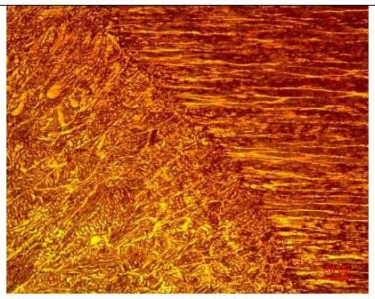	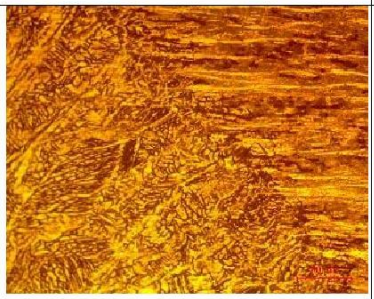	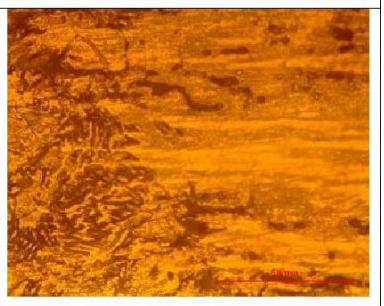

6	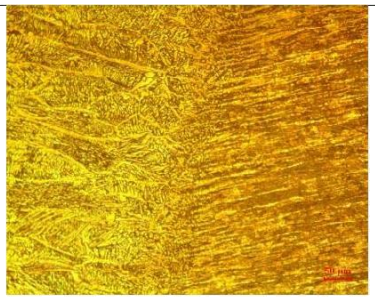	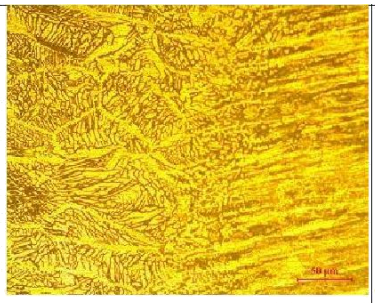	
7	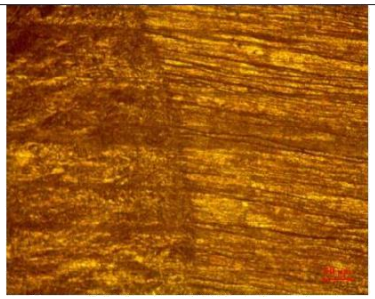	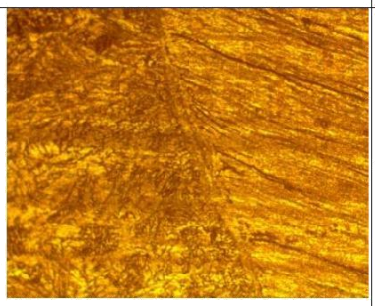	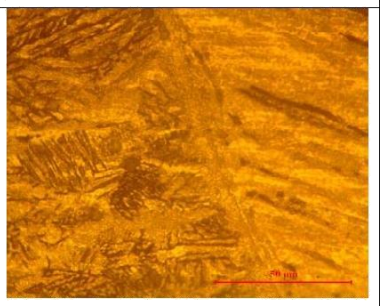
8	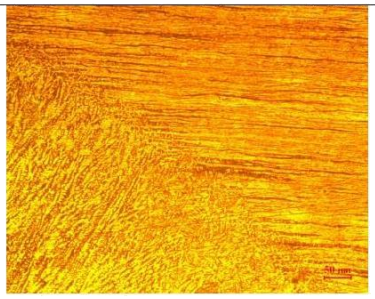	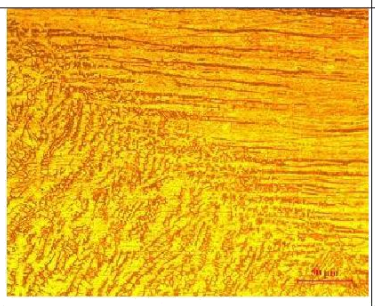	
9	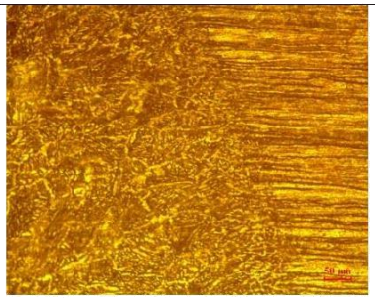	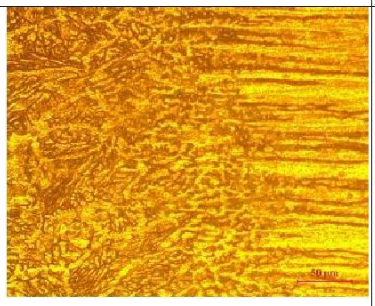	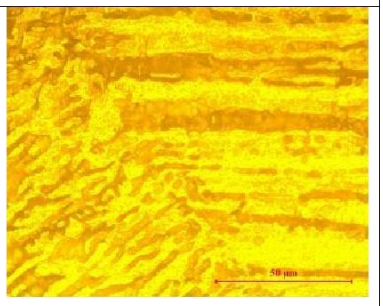
10	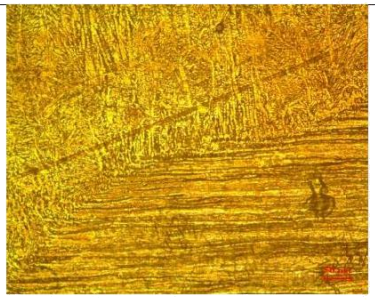	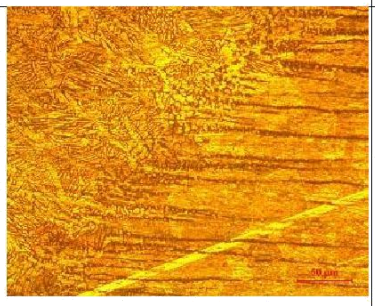	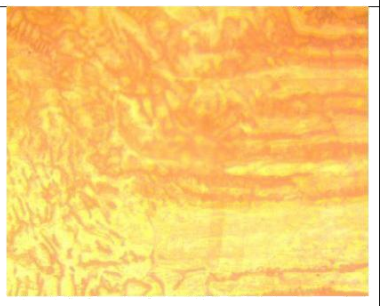
11	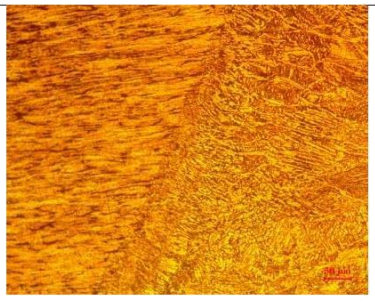		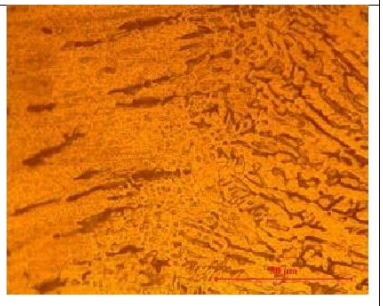

12	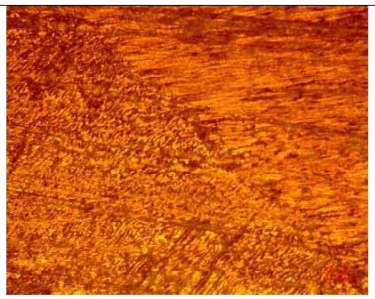	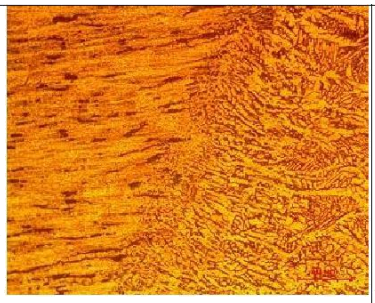	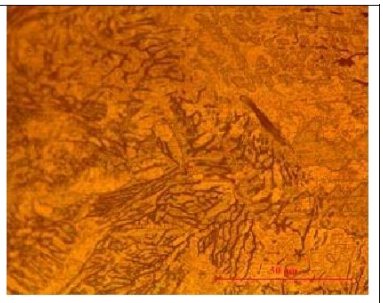
13	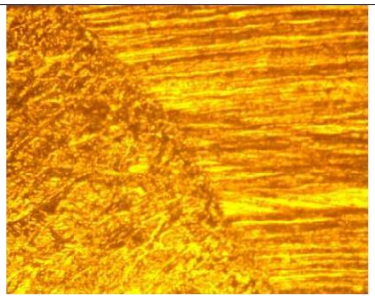	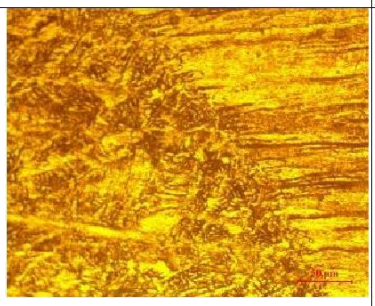	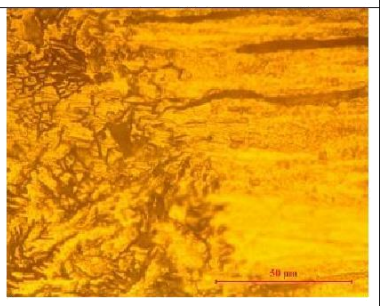
14			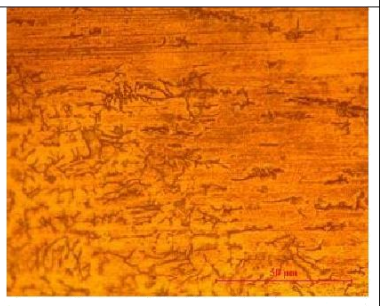
15	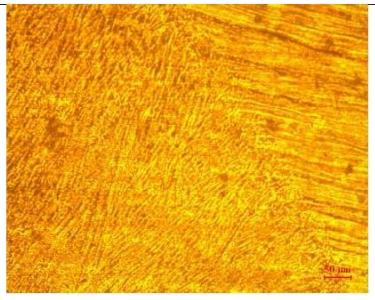	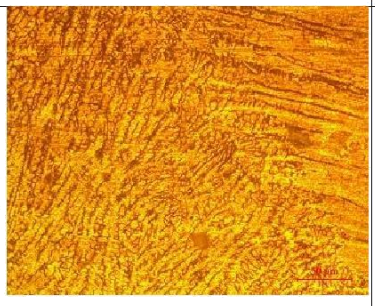	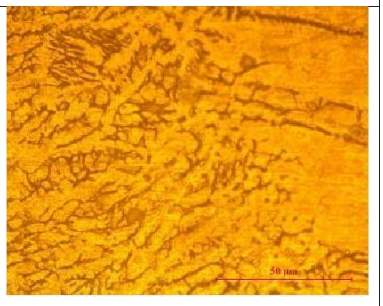
16	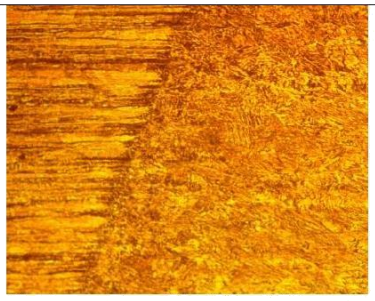	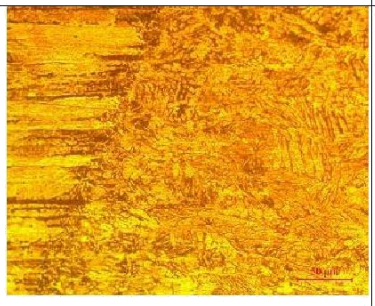	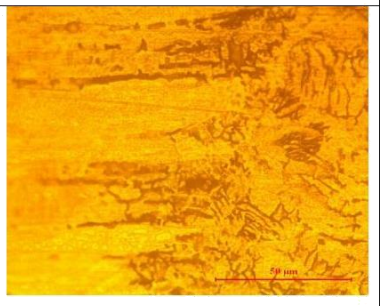
17	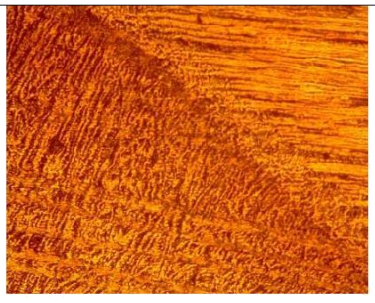	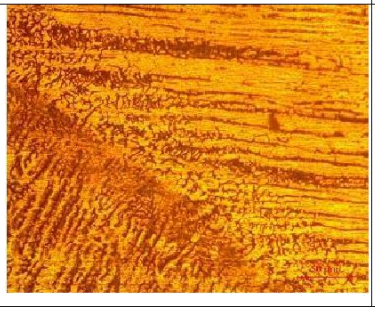	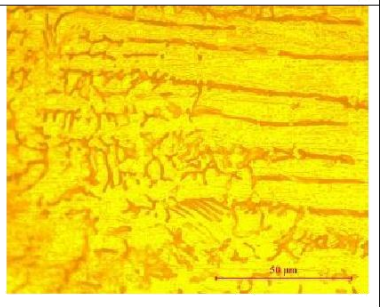

18	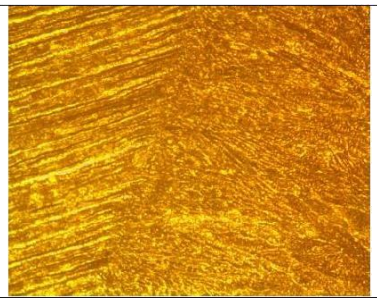	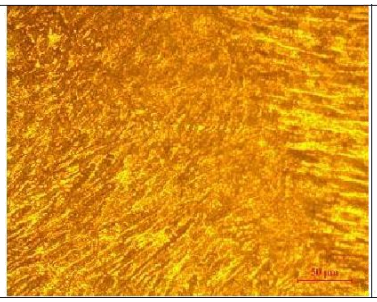	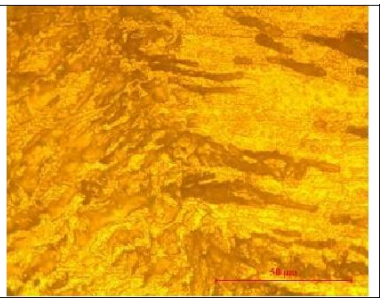

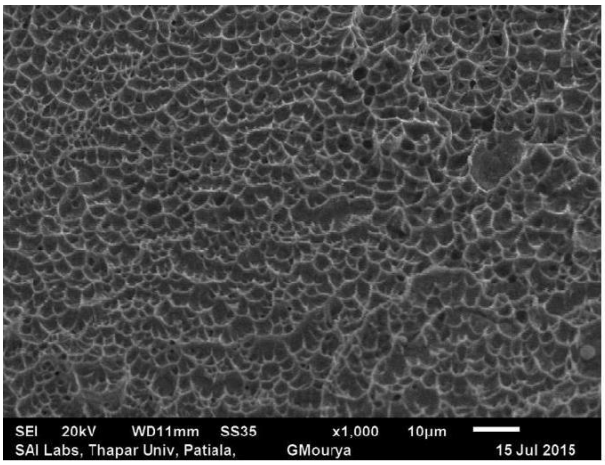

a

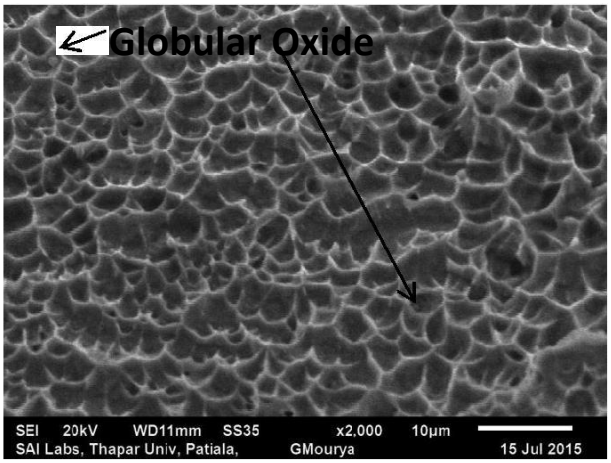

b

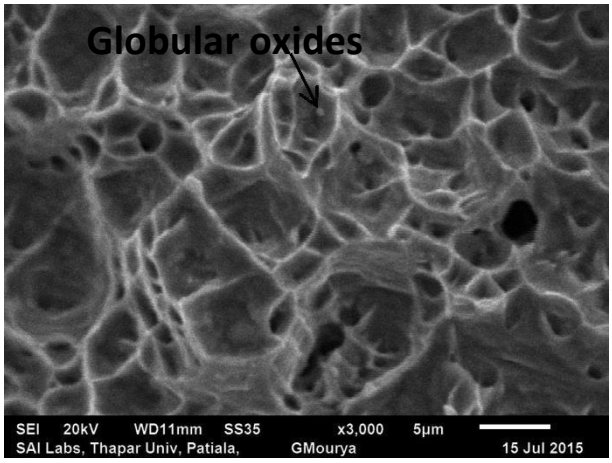

c

Figure 4.13: SEM images of fractured impact toughness sample having highest toughness at room temperature at a magnification of a) 1000X b) 2000X c) 3000X

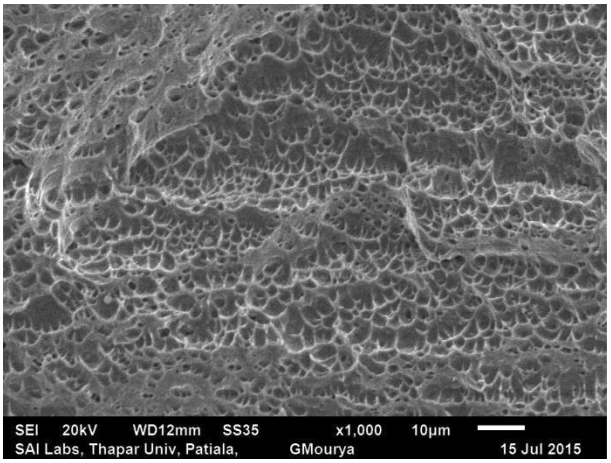

a

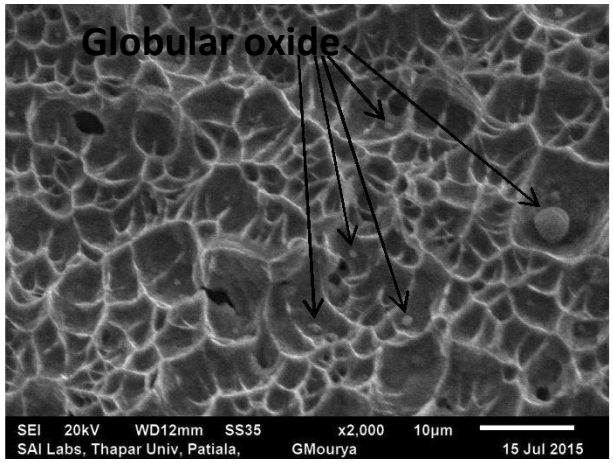

b

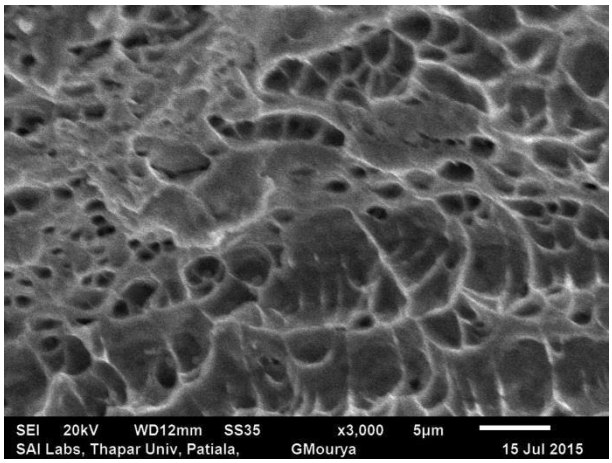

c

Figure 4.14: SEM images of fractured impact toughness sample having lowest toughness at room temperature at a magnification of a) 1000X b) 2000X c) 3000X

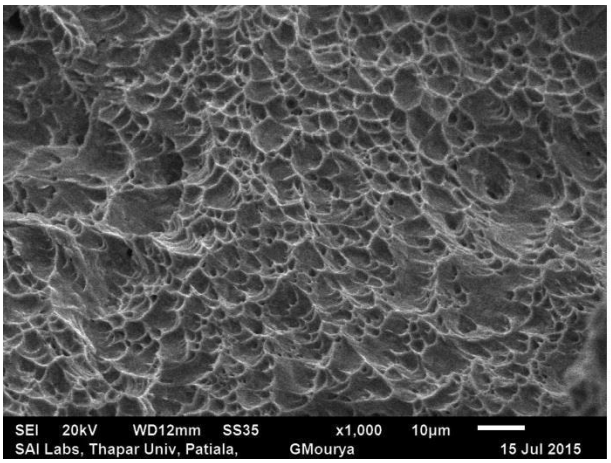

a

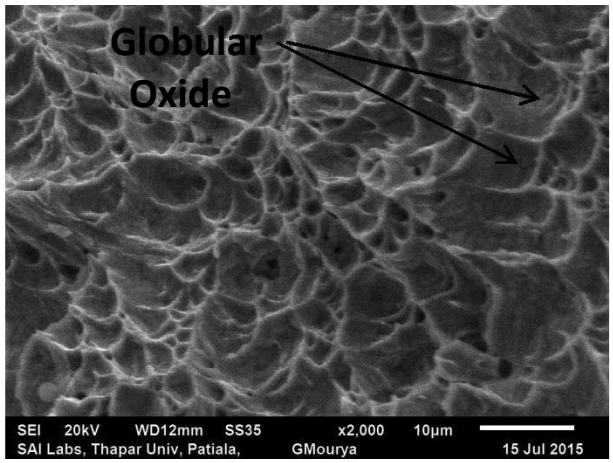

b

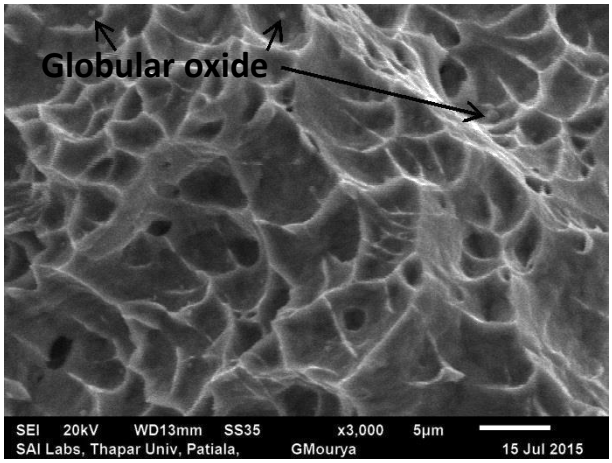

c

Figure 4.15: SEM images of fractured impact toughness sample having highest toughness at – 20℃ at a magnification of a) 1000X b) 2000X c) 3000X

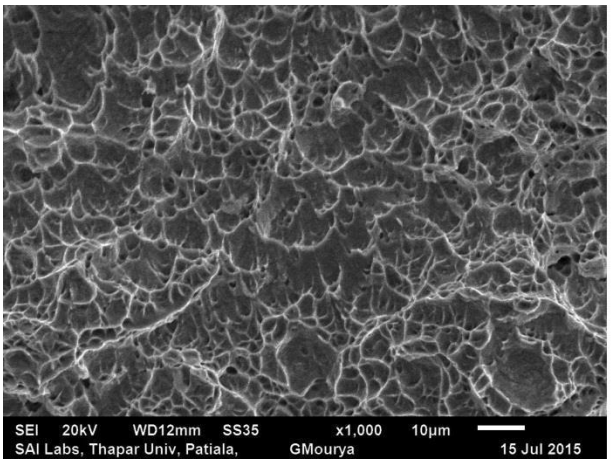

a

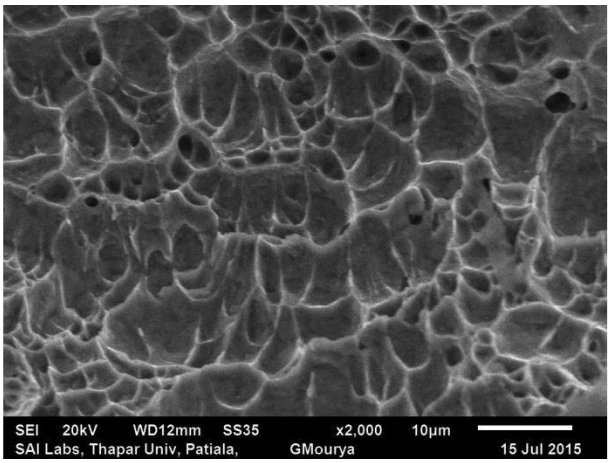

b

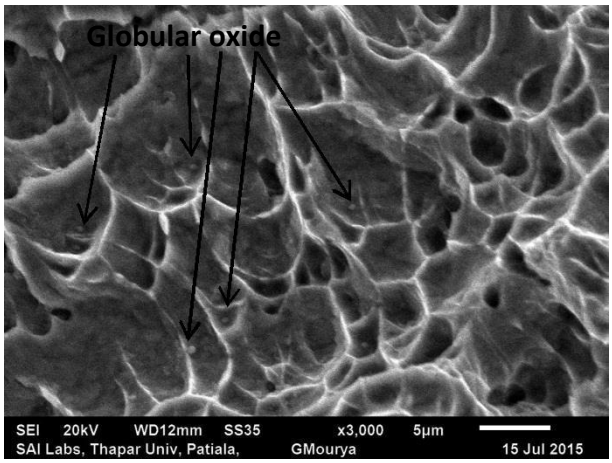

c

Figure 4.16: SEM images of fractured impact toughness sample having lowest toughness at – 20℃ at a magnification of a) 1000X b) 2000X c) 3000X

Figure 4.13 to 4.16 shows the SEM images of fractured impact toughness samples. Figure 4.13 and 4.14 are images of samples tested at room temperature. Figure 4.15 and 4.16 are images of samples tested at below room temperature. Samples are observed at the magnification of 1000X, 2000X and 3000X. Dimples of different shapes and sizes are observed in the SEM images of fractured specimens which shows that mode of fracture in samples is ductile. Dimples in figure 4.13 are smaller and shallower than in figure 4.14 which represents higher ductility for samples showed in figure 4.13. Similar trend is showed for samples tested at – 20℃, size of dimples in figure 4.15 is also smaller than in figure 4.16. Globular oxides are present in the fractured samples; these oxides are form of inclusion. Globular oxides are labelled in figure of fractured samples (figure 4.13 to 4.16), site of these oxides act as tension stress raiser, globular oxides also acts crack nucleators and promote cracks. Increase in oxide inclusion results in decreased strength of material.

Chapter 5

Conclusions and Scope for Future Work

5.1 Introduction

This chapter discusses the conclusions of the experiments done during this study. Scope for future studies on welding of austenitic stainless steel is also discussed in this factor. Effect of input parameters on properties like impact toughness at room temperature and below room temperature, distortion, microhardness of fusion zone and heat affected zone are concluded in this chapter.

5.2 Conclusions

- Distortion in welds is significantly affected by current voltage and edge including angle. Distortion in welds first increased with increase in current and then decreased with further increase in current. Distortion in welds first decreased with increase in voltage. Higher distortion is showed by the samples that are weld at the higher level of edge including angle. Interpass temperature and gas flow rate has not significantly affected the distortion and distortion increased with increase in the gas flow rate increase. The optimum value of distortion is 4.905 ± 0.694 degree at 220 A current, 24 V of voltage and 60˚of edge including angle.
- Impact toughness of welds at room temperature is significantly affected by the current and voltage. High impact toughness is increased with increase in current and voltage. Impact strength is increased with increase in gas flow rate and decreased with increase in interpass temperature. Impact toughness is first increased with increase in edge including angle and then decreased. The optimum value of toughness at room temperature is 179.93 ± 10.51 J at 220 A current and 26 V of voltage.
- Impact toughness of welds at -20˚C is significantly affected by current and voltage.

  Impact toughness is decreased with decrease in temperature. Toughness is increased with increase in current, voltage and gas flow rate. Toughness is decreased with

decrease in interpass temperature. Increase in edge including angle initially results in increase in toughness value and then decreased. Optimum value of impact toughness at below room temperature is 136 ± 7.27 J at 220A current and at 26 V of voltage.

- Microhardness of fusion zone is significantly affected by the voltage, current and interpass temperature. Microhardness of fusion zone is increased with increase in interpass temperature and voltage. Microhardness is first increased and then decreased with increase in current. Gas flow rate and edge including angle have not much effect on the microhardness of fusion zone. Optimum value of microhardness at fusion zone is 312 ± 53.34 HVN at 200 A current, 24 V of voltage and 100˚C of interpass temperature. Microhardness of heat affected zone is significantly affected by the current, voltage and interpass temperature. Optimum microhardness of heat affected zone is 316.26 ± 29.10 HVN at 200 A current, 24 V of voltage and 100˚C of interpass temperature.
- Optical micrographs showed that grain growth is perpendicular to fusion boundary because of high thermal gradient. Solidification mode is changes from planar to cellular to dendritic from base metal to dendrite. Dendrites of delta ferrite are present in austenite matrix.
- SEM images of fractured impact toughness specimens showed dimples of different shape and sizes which represents that mode of fracture in samples is ductile. SEM images shows presence of globular oxides, which act as stress concentrator.

5.3 Scope for Future Work

- Bending test, corrosion test and non-destructive test like radiography testing, ultrasonic testing of welds can be done to study the properties and quality of welds.
- Effect of different fluxes can be studied on austenitic stainless steel using activated metal inert gas welding.
- Empirical modelling, finite element modelling of the multipass welding process can be done for better understanding of the process.
- Optimisation of process parameter can be done using various optimisation techniques like fuzzy logic, response surface methodology, generic algorithms etc.

References

- Aghakhani, M; Mehrdad, E; Hayati, E. (2011) Parametric optimization of gas metal arc welding process by taguchi method on weld dilution. *International Journal of Modeling and Optimization*, 1(3): 216 – 220.

- Bhattacharya, A.; Bera, T.K. (2014) Development of automatic GMAW setup for process improvements: Experimental and modelling approach. *Materials and Manufacturing Processes*, 29 (8): 988 – 995.

- Bhattacharya, A; Bera, T.K; Suri, V.K. (2014) Influence of heat input in automatic gmaw: penetration prediction and microstructural observation.

Materials and Manufacturing Processes, 29(10): 1210 – 1218.

- Folkhard, E. (1988) Welding Metallurgy of Stainless Steels, Springer-Verlag/Wien, Austria.

- Furusawa, K; Yasuda, K. (2009) Study on gas metal arc welding procedure of stainless steel. *Welding International*, 14(9): 688 – 694.

- Galvis, A.R.; Hormaza, W. (2011) Characterization of failure modes for different welding processes of AISI/SAE 304 stainless steels, *Engineering Failure Analysis*, 18: 1791–1799.

- Ghosh, A; Mallik A.K. (2008) Manufacturing Science, East-West Press Private Limited, New Delhi-2008.

- Giridharan, P. K.; Murugan, N. (2009) Optimization of pulsed GTA welding process parameters for the welding of AISI 304L stainless steel sheets, *International Journal of Advanced Manufacturing Technology*, 40: 478–489.

- Gouveia, R. R. D.; Pukasiewicz, A. G. M.; Capra, A.R.; Henke, S. L.; Okimoto, P.C. (2015) Effect of interpass temperature on microstructure, impact toughness and fatigue crack propagation in joints welded using the GTAW process on steel ASTM A743-CA6NM, *Welding International*, 29(6): 433-440.

- Gulenç, B; Develib, K; Kahramanc, N; Durgutlua A. (2005) Experimental study of the effect of hydrogen in argon as a shielding gas in MIG welding of

austenitic stainless steel. *International Journal of Hydrogen Energy*, 30: 1475 – 1481.

- Khanna, O.P. (1986) Welding Technology, Dhanpat Rai & Sons, New Delhi.
- Kou, S. (2003) Welding Metallurgy, John Wiley & Sons, New Jersey.
- Kumar R.; Bhattacharyaa A.; Bera, T.K. (2014) Mechanical and metallurgical studies in double shielded gmaw of dissimilar stainless steels, *Materials and Manufacturing Processes,* available online, DOI:10.1080/10426914.2014.994760.
- Kumar, L.S; Verma, S. M; Suryanarayana, B; Kumar, P.K. (2012) Analysis of welding characteristics on stainless steel for the process of tig and mig with dye penetrate testing. *International Journal of Engineering and Innovative Technology*, 2(1): 283– 290.
- Kumar, P; Batish, A; Bhattacharya, A and Duvedi, R.K. (2011) Effect of process parameters on microhardness and microstructure of heat affected zone in submerged arc welding. *Proceedings of The Institution Of Mechanical Engineers, Part B: Journal of Engineering Manufacture*, 225: 711–721.
- Kumar, S; Shahi, A.S. (2011) Effect of heat input on the microstructure and mechanical properties of gas tungsten arc welded AISI 304 stainless steel joints, *Materials and Design*, 32: 3617–3623.
- Kumar, S; Shahi, A.S. (2014) On the Influence of Welding Stainless Steel on Microstructural Development and Mechanical Performance, *Materials and Manufacturing Processes*, 29(8): 894 – 902.
- Kyriakongonas, A. P.; Papazoglou, V. J.; Pantelis, D. I. (2011) Complete investigation of austenitic stainless steel multi-pass welding, *Ships and Offshore Structures*, 6(1-2): 127-144.
- Mirshekari, G.R.; Avakoli, E; Atapour, M; Sadeghian, B. Microstructure and corrosion behavior of multipass gas tungsten arc welded 304L stainless steel. *Materials and Design* , 55: 905– 911.
- Murugan, N; Parmar, R.S. (1994) Effect of process parameter on the geometry of the bead in automatic surfacing of stainless steel. *Journal of Material Process Technology*, 41: 381 – 398.

- Murugan, S; Rai, S.K.; Kumar, P.V; Jayakumar, T; Raj, B; Bose, M.S.C. (2001) Temperature distribution and residual stresses due to welding type 304 stainless steel and low carbon steel weld pads. *International Journal of Pressure Vessel and Piping*, 78: 307–317

- Nanda, A; Kumar, S; Nanda G. (2013) Optimizing the mechanical properties of AISI 304 steel in gas metal arc welding process. *International Journal on Emerging Technologies* , 4(1): 112-122.

- Niagaj, J. (2014) Ways to improve the efficiency of welding stainless steel, *Welding International*, 28(1):45-53.

- Saha, S.; Mukherjee, M.; Pal, T.K. (2014) Microstructure, texture, and mechanical property analysis of gas metal arc welded aisi 304 austenitic stainless steel, *Journal of Materials Engineering and Performance*, 24: 1125–1139.

- Sathiya, P; Ajith, M; Soundararajan, R. (2013) Genetic algorithm based optimization of the process parameters for gas metal arc welding of AISI 904 L stainless steel. *Journal of Mechanical Science and Technology*, 27: 2457– 2465.

- Srinivasan, K; Balasubramanian, V. (2011) Effect of Heat Input on Fume Generation and Joint Properties of Gas Metal Arc Welded Austenitic Stainless Steel. *Journal of Iron and Steel Research, International*, 18(10): 72-79.

- Tathgir, S; Bhattacharya, A. (2015) Activated-TIG welding of different steels: influence of various flux and shielding gas, *Materials and Manufacturing Processes*, available online, DOI: 10.1080/10426914.2015.1037914.

- Tusek, J; Suban, M. (2000) Experimental research of the e€ect of hydrogen in argon as a shielding gas in arc welding of high-alloy stainless steel, *International Journal of Hydrogen Energy*, 25: 369 –376.

- Vasantharaja, P.; Vasudevan M., Palanichamy, P. (2014) Effect of welding processes on the residual stress and distortion intype 316LN stainless steel weld joints, *Journal of Manufacturing Processes*, available online, http://dx.doi.org/10.1016/j.jmapro.2014.09.004.

- Weman, K. Lindean, G. (2006) MIG Welding Guide, Woodhead Publishing Limited, England.

- Yılmaz, R.; Tümer, M. (2013) Microstructural studies and impact toughness of dissimilar weldments between AISI 316 L and AH36 steels by FCAW, *International Journal of Advanced Manufacturing Technology*, 67:1433–1447.

Web references

- http://mechanicalinventions.blogspot.in/2012/11/gas-metal-arc-welding-gmaw-or-mig.html on 13/12/2014 at 11:45 AM
- http://www.weldguru.com/Mig.html on 13/12/2014 at 11:45 AM